APPENDIX A

```
%transient temperature distribution for flat plate
n=input('n=');
Kt=input('thermal conductivit=');
al=input('thermal diffusivity=');
h=zeros(n,n);
h(:,1)=200;
h(:,n)=200;
h(1,:)=200;
h(n,:)=200;
gg=h;
for m=2:n-1
   for w=2:n-1
h(m,w)=30;
end
end
 p=zeros(n,n);
 TT=p+h
  for j=1:10
ht=30;                    %h=hu+hl
Tf=15;                    %fluid temperatur
dt=1*60;
x=0.1;
d=0.125;
R=2;
Fo=al*dt/x^2;             %fourier number
Bi=ht*x/Kt;               %Biot number
 for m=2:8
   for n=2:8
p(m,n)=(1-4*Fo-R*Fo*Bi)*TT(m,n)+Fo*(TT(m+1,n)+TT(m-
1,n)+TT(m,n+1)+TT(m,n-1))+(R*Fo*Bi)*Tf;        %eq(1)
end
end
   j
TT=p+gg

end

%%%%%%%%%%%%%%%%%%%%%%%%%%%%%%%%%%%%%%%%%%%%%%%
%%%%%%%%%%%%%%%%%%%%%%%%%%%%%%
%transient temperature distribution for T-element
n=input('n=');
Kt=input('thermal conductivity=');
al=input('thermal diffusivity=');
h=zeros(n,n);
h(:,1)=200;
h(:,n)=200;
h(1,:)=200;
h(n,:)=200;
gg=h;
```

```
for m=2:n-1
   for w=2:n-1
h(m,w)=30;
end
end
 p=zeros(n,n);
 TT=p+h
  for j=1:10
ht=30;                    %h=hu+hl
Tf=15;                    %fluid temperatur
dt=1*60;
x=0.1;
d=0.125;
R=2;                      %Ratio
Fo=al*dt/x^2;              %fourier number
Bi=ht*x/Kt;                %Biot number
 for m=2:8
   for n=2:8
p(m,n)=(1-4*Fo-R*Fo*Bi)*TT(m,n)+Fo*(TT(m+1,n)+TT(m-
1,n)+TT(m,n+1)+TT(m,n-1))+(R*Fo*Bi)*Tf;        %eq(1)
end
end
hu=20;
Biu=hu*x/Kt;
n=5;
for m=2:8
 p(m,n)=(1-4*Fo-R*Fo-R*Fo*Biu)*TT(m,n)+Fo*(TT(m+1,n)+TT(m-
1,n)+TT(m,n+1)+TT(m,n-1))+(R*Fo*Biu)*Tf;    %eq(2)
end
   j

 TT=p+gg
n=9;
h1=zeros(n,n);
h1(:,1)=200;
h1(:,n)=200;
h1(1,:)=40;
for mm=1:9
        h1(9,mm)=TT(mm,5);
end
for m=2:n-1
   for w=2:n-1
h1(m,w)=30;
end
end
 for j=1:10
 for m=2:8
   for n=2:8
p1(m,n)=(1-4*Fo-R*Fo*Bi)*TT(m,n)+Fo*(TT(m+1,n)+TT(m-
1,n)+TT(m,n+1)+TT(m,n-1))+(R*Fo*Bi)*Tf;
```

```
end
end

  j;

end
end

for m=2:8
    for n=2:8
p1(m,n)=+Fo*(TT(m+1,n)+TT(m-1,n)+TT(m,n+1)+TT(m,n-1))+(1-4*Fo)*TT(m,n);
%eq(3)
end
end
%%%%%%%%%%%%%%%%%%%%%%%%%%%%%%%%%%%%%%%%%%%
%%%%%%%%%%%%%%%%%%%%%%%%%%%%%%%%%%%%%
%transient temperature distribution for stiffened structure plate
n=input('n=');
Kt=input('thermal conductivit=');
al=input('thermal diffusivity=');
h=zeros(n,n);
h(:,1)=200;
h(:,n)=200;
h(1,:)=200;
h(n,:)=200;
gg=h;
for m=2:n-1
   for w=2:n-1
h(m,w)=30;
end
end
 p=zeros(n,n);
 TT=p+h

ht=30;                          %h=hu+hl
Tf=15;                          %fluid temperatur
dt=1*60;
x=0.2;
d=0.125;
R=2;
Fo=al*dt/x^2;
Bi=ht*x/Kt;                     %Biot number
 for j=1:10
for m=2:16
   for n=2:16
p(m,n)=(1-4*Fo-R*Fo*Bi)*TT(m,n)+Fo*(TT(m+1,n)+TT(m-
1,n)+TT(m,n+1)+TT(m,n-1))+(R*Fo*Bi)*Tf;        %eq(1)
end
end
hu=20;
```

```
Biu=hu*x/Kt;
for n=5:4:13
for m=2:16
 p(m,n)=(1-4*Fo-R*Fo-R*Fo*Biu)*TT(m,n)+Fo*(TT(m+1,n)+TT(m-
1,n)+TT(m,n+1)+TT(m,n-1))+(R*Fo*Biu)*Tf;    %eq(2)
end
end
z=p;
j
TT=z+gg
end
```

Chapter Five

Conclusions and Recommendations For Future Work

5.1:Conclusions

The following conclusions are obtained from the analysis of the present results.

1. The material property has an effect on the shape of the temperature distribution for T-element and stiffened plate but has no effect on flat plate.
2. The concaveness of the temperature profile for flat plate does not occur when thermal conductivity is varied.
3. The concaveness of the temperature profile for T-element and stiffened structure occurs at the coupling mesh when thermal conductivity is varied.
4. The value of thermal conductivity for T-element and stiffened structure plate has an effect on the shape of the concaveness. The concaveness is downward for large value of thermal conductivity and it's upwards for small values of thermal conductivity.
5. Concaveness occurs at each coupling mesh for stiffened structure plate.
6. The concaveness at the coupling mesh, which may cause thermal stresses, must be considered in the selection of material.

5.2:Future Works

During the course of this research, there appear some aspects that can be further developed to enhance this work the following suggestions could serve as further topics of research with in the same field of this thesis

1. Introducing a new study includes the heat generation in the equation of energy balance and study the effect of thermal conductivity on the shape of temperature distribution for these cases.
2. The value of convection heat transfer coefficient can be changed to be appropriate to the environment to which the structure subjected.
3. It will be interesting to study temperature distribution on the same structures by using finite element analysis.
4. Experimental studies of temperature distribution on the structures.

Chapter Four

Calculations, Results and Discussion

4.1:Calculations

Sample of a different structures will mentioned below for different boundary conditions such as

4.1.1:For Flat Plate

Consider the flat plate shown in figure 3-5 and the boundary conditions are assumed to be:

1-All boundaries at $T = 200\,\text{C}°$

2-the plate initially at $T = 30\ \text{C}°$

3-fluid temperature or environment temperature $T_f = 15\,\text{C}°$

4-convection-heat transfer coefficient for upper surface is $h_u = 20\,\text{W/m}^2.\,\text{C}°$

5-convection-heat transfer coefficient for lower surface is $h_l = 10\ \text{W/m}^2.\,\text{C}°$

6-different type of material will be used as shown in the table:

Metal	K = W/m .C°	α = m²/s
Copper	386	11.234×10^{-5}
Nickel steel	73	2.026×10^{-5}
Glass fiber	0.038	22.6×10^{-7}

The properties of the material will be taken from Ref. [26]

7- the value of Δt and Δx are selected such that they must satisfy the stability criteria. Since

$$Fo = \frac{\alpha \Delta t}{\Delta x^2}$$

$$Bi = \frac{h\Delta x}{K}$$

$$R = \frac{\Delta x}{d}$$

And the stability criteria is

$$Fo\,(4 + R\,Bi) \le 1$$

8- the thickness of the plate assumed to have a value of $d = 0.1\,\text{m.}$ or $d = 0.125\,\text{m.}$ and the length of the plate have a value $L = 0.8m$ or $L = 1.6m$

9-the grid space was chosen to be $\Delta x = 0.1\,\text{m.}$ or $\Delta x = 0.2\,\text{m}$ depending on the stability limit

10-the time increment was chosen to be $\Delta t = 1\,\text{min.}$

By knowing the initial temperatures at time=0 the temperature at the next time step can be calculated from equation (3-39)

$$T_{m,n}^{j+1} = (1 - 4Fo - RFoBi)T_{m,n}^{j} + Fo\left(T_{m+1,n}^{j} + T_{m-1,n}^{j} + T_{m,n+1}^{j} + T_{m,n-1}^{j}\right) + RFoBiTf$$

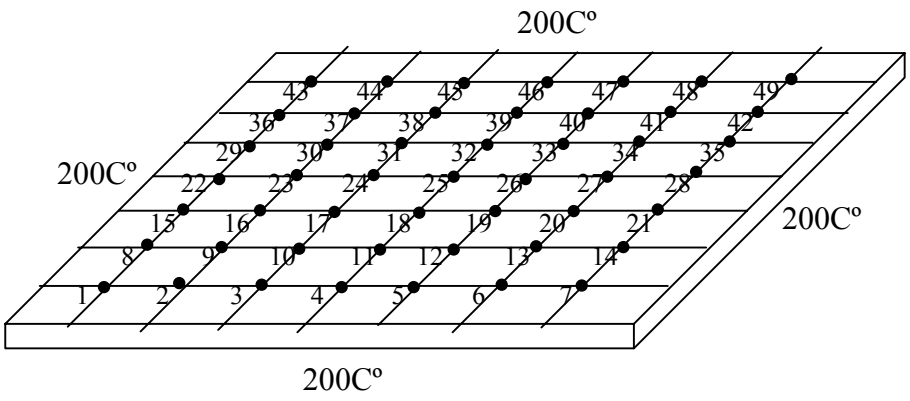

Figure 4-1: Nodal distribution in flat plate

Put

$$a = (1 - 4Fo - RF0Bi)$$

$$a1 = Fo$$

$$a2 = RFoBiT_f$$

For node 1

$$T_1^{j+1} = a\,T_1^{j} + a1\left(T_2^{j} + 200 + T_8^{j} + 200\right) + a2$$

For node 2

$$T_2^{j+1} = a\,T_2^{j} + a1\left(T_3^{j} + T_1^{j} + T_9^{j} + 200\right) + a2$$

For node 3

$$T_3^{j+1} = aT_3^{j} + a1\left(T_4^{j} + T_2^{j} + {}_{10}^{j} + 200\right) + a2$$

For node 4

$$T_4^{j+1} = aT_4^j + a1\left(T_5^j + T_3^j + T_4^j + 200\right) + a2$$

For node 5

$$T_5^{j+1} = aT_5^j + a1\left(T_6^j + T_4^j + T_{12}^j + 200\right) + a2$$

For node 6

$$T_6^{j+1} = aT_6^j + a1\left(T_7^j + T_5^j + T_{13}^j + 200\right) + a2$$

In the same way continue for all nodes in the plate to get the temperature distribution for the whole plate

4.1.2:For T-element

Consider the T-element shown in the figure (3-6) and the boundary conditions are assumed to be:

1-All boundaries at $T = 200\,\text{C}°$

2-the plate initially at $T = 30\ \text{C}°$

3-fluid temperature or environment temperature $T_f = 15\,\text{C}°$

4-convection-heat transfer coefficient for upper surface is $h_u = 20\,\text{W/m}^2.\,\text{C}°$

5-convection-heat transfer coefficient for lower surface is $h_l = 10\ \text{W/m}^2.\,\text{C}°$

6-different type of material will be used as shown in the table:

Metal	K = W/m .C°	α = m²/s
Copper	386	11.234×10^{-5}
Aluminum	204	8.418×10^{-7}
Nickel steel	73	2.026×10^{-5}
Ni-Cr	17	0.444×10^{-5}
Asbestos	0.154	3.3×10^{-7}
Glass fiber	0.038	22.6×10^{-7}

The properties of the material will be taken from Ref. [26]

7- the value of Δt and Δx are selected such that they must satisfy the stability criteria. Since

$$Fo = \frac{\alpha \Delta t}{\Delta x^2}$$

$$Bi = \frac{h \Delta x}{K}$$

$$R = \frac{\Delta x}{d}$$

And the stability criteria for T-element are:

$$Fo\,(4 + R\,Bi) \le 1 \qquad \text{Equation (3-40)}$$

$$Fo(4 + R + RBi_u) \le 1 \qquad \text{Equation (3-51)}$$

8- the thickness of the plate assumed to have a value of $d = 0.1\,\text{m.}$ or $d = 0.125\,\text{m}$ and the length of the plate have a value $L = 0.8m$ or $L = 1.6m$

9-the grid space was chosen to be $\Delta x = 0.1\,\text{m.}$ or $\Delta x = 0.2\,\text{m}$ depending on stability limit

10-the time increment was chosen to be $\Delta t = 1\,\text{min.}$

By knowing the initial temperatures at time=0 the temperature at the next time step can be calculated from equation (3-50). Since

a - $$T_{m,n}^{j+1} = (1 - 4Fo - RFoBi)T_{m,n}^{j} + Fo\left(T_{m+1,n}^{j} + T_{m-1,n}^{j} + T_{m,n+1}^{j} + T_{m,n-1}^{j}\right) + RFoBiTf$$

b-

$$T_{m,n}^{j+1} = (1 - 4Fo - RFo - RF0Bi_u)T_{m,n}^{j} + Fo(T_{m+1,n}^{j} + T_{m-1,n}^{j} + T_{m,n+1}^{j} + T_{m,n-1}^{j} + RFoT_{l+1} + RFoBi_lT_f$$

c- $$T_{n,l}^{j+1} = (1 - 4Fo)T_{n,l}^{j+1} + Fo\left[T_{n+1,l}^{j} + T_{n-1,l}^{j} + T_{n,l}^{j} + T_{n,l-1}^{j}\right]$$

Put:

$$a = (1 - 4Fo - RF0Bi)$$

$$a1 = Fo$$

$$a2 = RFoBiT_f$$

$$b = (1 - 4Fo - RFo - RFoBiu)$$

$$b1 = Fo$$

$$b2 = RFoT_{l+1}$$

$$b3 = RFoBiuT_l$$

$$c = (1 - 4Fo)$$

$$c1 = Fo$$

The temperature at each node in the skin can be calculated by using system of equations.

Equation (3-39):

For node 1

$$T_1^{j+1} = a\,T_1^j + a1\left(T_2^j + 200 + T_8^j + 200\right) + a2$$

For node 2

$$T_2^{j+1} = a\,T_2^j + a1\left(T_3^j + T_1^j + T_9^j + 200\right) + a2$$

For node 3

$$T_3^{j+1} = aT_3^j + a1\left(T_4^j + T_2^j + {}_{10}^j + 200\right) + a2$$

For node 5

$$T_5^{j+1} = aT_5^j + a1\left(T_6^j + T_4^j + T_{12}^j + 200\right) + a2$$

For node 6

$$T_6^{j+1} = aT_6^j + a1\left(T_7^j + T_5^j + T_{13}^j + 200\right) + a2$$

For node 7

$$T_7^{j+1} = aT_7^j + a1(200 + T_6^j + T_{14}^j + 200) + a2$$

Equation (3-50):

The temperature in the coupling mesh is calculated as shown

For node 4

$$T_4^{j+1} = bT_4^j + b1(T_5^j + T_3^j + T_{11}^j + 200) + b2 + b3$$

For node 11

$$T_{11}^{j+1} = bT_{11}^j + b1(T_{12}^j + T_{10}^j + T_{18}^j + T_4^j) + b2 + b3$$

For node 18

$$T_{18}^{j+1} = bT_{18}^j + b1(T_{19}^j + T_{17}^j + T_{28}^j + T_{11}^j) + b2 + b3$$

In the same way continue for all nodes in the skin to get the temperature distribution for the whole skin of T-element.

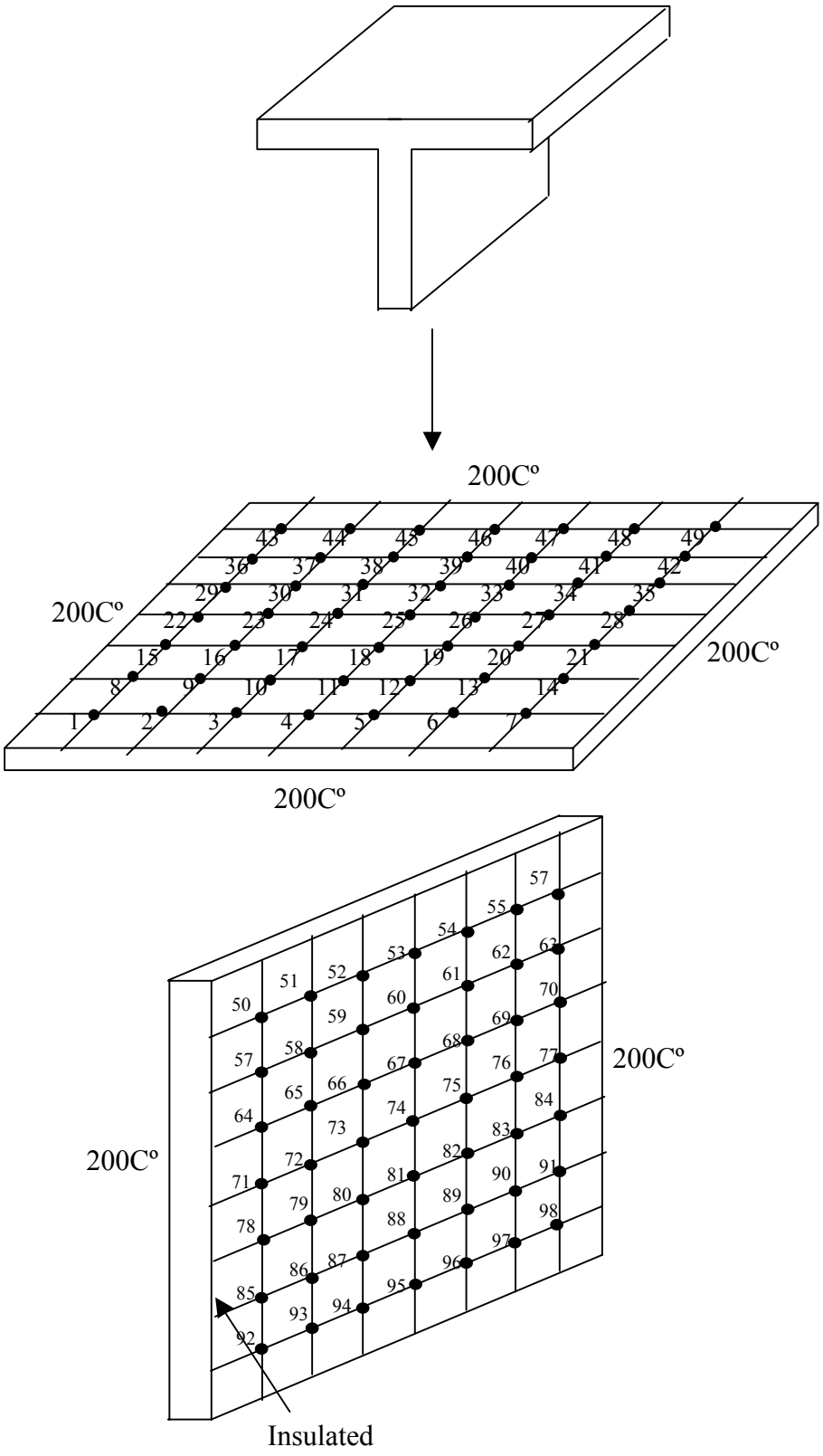

Figure 4-2: Nodal distribution in T-element

3-For Stiffened Structure Plate

The same procedure will be made to find the temperature distribution over the skin of the stiffened structure plate but equation (3-50) will be used at each coupling mesh.

4.2:Results and Discussion

The research cases are shown in fig. 3-5, 3-6 and 3-8. The calculations of temperature distribution for each increment of time and that for different types of thermal conductivity were made.

The partial differential equation for each case was obtained from the energy balance and that was solved by finite difference method. The assumptions and boundary conditions were considered. For each equation the values of $(\Delta x)$and (Δt) were chosen so that they must be satisfy the stability limit. The temperature distribution for each increment of time (transient finite difference) was obtained by using a computer program.

The variation of temperature over the length of the plate i.e. (two dimensional plot) for different values of thermal conductivity of the material was plotted for a slice of the plate. Also contour plot was made for the whole plate to show the temperature distribution.

The bold line in the diagram (shown on top of each figure for each type of the structure) marks the location where the temperature distribution was plotted. Any other location could have been chosen since the shape of the temperature profile is not affected by the location where the temperature distribution acts. The legend beside the figure shows the time increment for each plot. The results shows

4.2.1:Flat Plate

For the flat plate shown in figure 3-5. The rectangular plate of thickness (d) being subjected to convection from the upper and lower surfaces and to conduction from both (x) and (y) directions since the plate having a value initially at (30C^{o}) and the boundaries being maintained at (200C^{o}) i.e. the plate has a symmetrical boundary condition. Equation (3-39) was used to find the temperature distribution over the whole plate.

Figure 4-1 shows the variation of temperature with plate length at different time increment. The temperature drops at both sides towards the neighbor node and remain almost constant at the center of the plate (the flat portion).

Figures 4-2 and 4-3 show that the variations of the time increment and that of material properties do not change the flatness of the curve.

4.2.2:T-element

For the T-element (skin-web) shown in fig. 3-6 in which the coupling mesh was subjected to convection at the upper surface and to conduction at the side and bottom surfaces. System of equations for the skin and coupling mesh were used to find the temperature distribution over the skin of T-element.

Figures 4-4, 4-5, 4-6 and 4-7 show the variation of temperature with plate length for each increment of time (1min).

It is seen that the curve at the region of (coupling mesh) was concaved downward until its bottom reaching to global minimum.

This global minimum is decreasing with the increasing of the time interval also the shape of the curve will be different for each type of the thermal conductivity because the thermal resistance due to conduction $\left(R_{cond}=\frac{\Delta x}{kA}\right)$ is less than thermal resistance due to convection $\left(R_{conv}=\frac{1}{hA}\right)$ for the same cross sectional area. Therefore the coupling mesh acts as a heat sink i.e. (heat sinking to the web).

Figures 4-5, 4-7 and 4-9 show the effect of using materials of different thermal conductivity for each plot. The general shape of the concaveness is maintained but the global minimum is affected. A lower value is obtained for higher thermal conductivity.

Figures 4-8 and 4-9 show the variation of the temperature with plate length for each increment of time.

It is seen that the curve at the region of (coupling mesh) was concaved upward until its top reaching to global maximum.

This global maximum is decreasing with the increasing of the time interval because the thermal resistance due to conduction is greater than thermal resistance due to convection for the same cross sectional area therefore coupling mesh acts as a heat source.

These effects that discussed above in (4.2.2) at the coupling mesh of the T-element structure will cause thermal stresses acting on this region and the structural material expands and contracts as shown in equation (c) in addition to the existing of mechanical stress. These stresses may cause mechanical failures in the structure. Therefore this effect must be taken into consideration in the design application.

4.2.3:Stiffened Structure Plate

Figure 3-8 shows integrally stiffened structure plate that has three coupling mesh. Figures 4-10, 4-11, 4-12 and 4-13 show the variation of temperature with plate length for integrally stiffened structure. It shows that the concaveness occurs at each coupling mesh and it occurs downwards but in fig 4-14 the concaveness occur upwards until its top reaching global maximum then it will be decreased for each increase of time interval. The global minimum at the middle web of the structure is higher than that of the other branches as shown in fig. 4-15.

4.3:Contour Plots

Temperature distribution for flat plate, T-element and integrally stiffened plate were plotted in contour.

a-<u>For flat plate</u>

Figure 4-18 shows the three-dimensional plot of temperature distribution over flat plate for (t=6min).

Figure 4-18a is the color region plot and figure 4-18b is the mesh plot.

It can be seen that the temperature profile was found to be a parabolic when viewed in both front and sidewise. The increase of time increment does not affect the flatness of the curve as shown in fig 4-19.

b-For T-element

Figure 4-20 shows the variation of temperature distribution over skin of the T-element in color region and mesh plot. Figure 4-20a shows that when progress towards the center of the skin of T-element. The temperature shape mode is decreasing when viewed in front view this is due to convection heat transfer effect. Therefore the trend of temperature profile in line (2) has greater than line (1) and so line (3) has greater than (2) until reach the center of the skin. As for the side view no concaveness is seen and the shape of the temperature profile is parabolic. This shows that the web has not affected on the profile viewed from side.

The line (ii) is greater than line (i) and so line (iii) is greater than line (ii). In the mathematical point of view coupling mesh cause concaveness and this appears when viewed frontally.

Figure 4-20b shows the temperature distribution as gray color region. The legend beside the figure shows the variation of temperature distribution.

Zone (1) shows the interaction between the two curves of the front and size view. Zone (2) shows the global minimum at the coupling mesh.

The corner in T-element is a point of interference between the two curves. Figure 4-21 shows the variation of temperature distribution over skin of T-element at different time increment (a, t=1;b, t=2;c, t=3min).

c-Stiffened Structure Plate

Figure 4-22 shows the temperature distribution for stiffened structure plate in gray color region and mesh plots. Figure 4-22a shows the temperature distribution as mesh. The concaveness is seen at each coupling mesh when viewed from the front. Also the temperature shape mode is decreasing when viewed in front view this is due to convection

heat transfer effect. Therefore the trend of temperature profile in line (2) has greater than line (1) and so line (3) has greater than (2) until reach the center of the skin

Figure (4-22b) shows the temperature distribution as color region. The legend beside the figure shows the variation of temperature distribution. Zone (1) shows the interaction between the two curves of the front and size view.

Zone (2) shows the concaveness of the curve and the global minimum at each coupling mesh. Figure 4-23 shows the variation of temperature distribution over skin of stiffened structure plate at different time increment (a, t=1;b, t=2;c, t=3min).

Figure 4-24 shows temperature distribution in skin of stiffened structure plate at (t=40min). The global minimum at the middle web of the structure is higher than that of the other branches.

4.4:Radiation Effects

As for the radiation effect on the different types of the structures.

Equation (3-61)

$q_{rad} = \sigma \varepsilon A(T_1^4 - T_2^4)$

Where $\sigma = 5.669 \times 10^{-8}$ W/m².k^4 Stefan-Boltzman constant.

$q_{conv} = hA(T - T_f)$

$T_f = 15\,\text{C}^\circ$ $A = 0.1 \times 0.1$ m²

$q_{conv} = 30 \times 0.1 \times 0.1(200 - 15)$

$q_{conv} = 55.5\,\text{W}$

Taking the Nickel as a sample for calculation of radiant heat

The Emissivity $\varepsilon = 0.1$ from Ref. [26]

$T_1 = 200 + 273 = 473\,\text{k}$ $T_2 = 15 + 273 = 288\,\text{k}$

$q_{rad} = 5.669 \times 10^{-8} \times 0.1 \times (0.1)^2 (473^4 - 288^4)$

$q_{rad} = 2.45\,\text{W}$

$$Error = \frac{q_{rad}}{q_{rad} + q_{conv}} \times 100\%$$

$$Error = \frac{2.45}{2.45 + 55.55} \times 100\% = 4.2\%$$

The calculation below show that the radiant heat can be neglected since the error is acceptable.

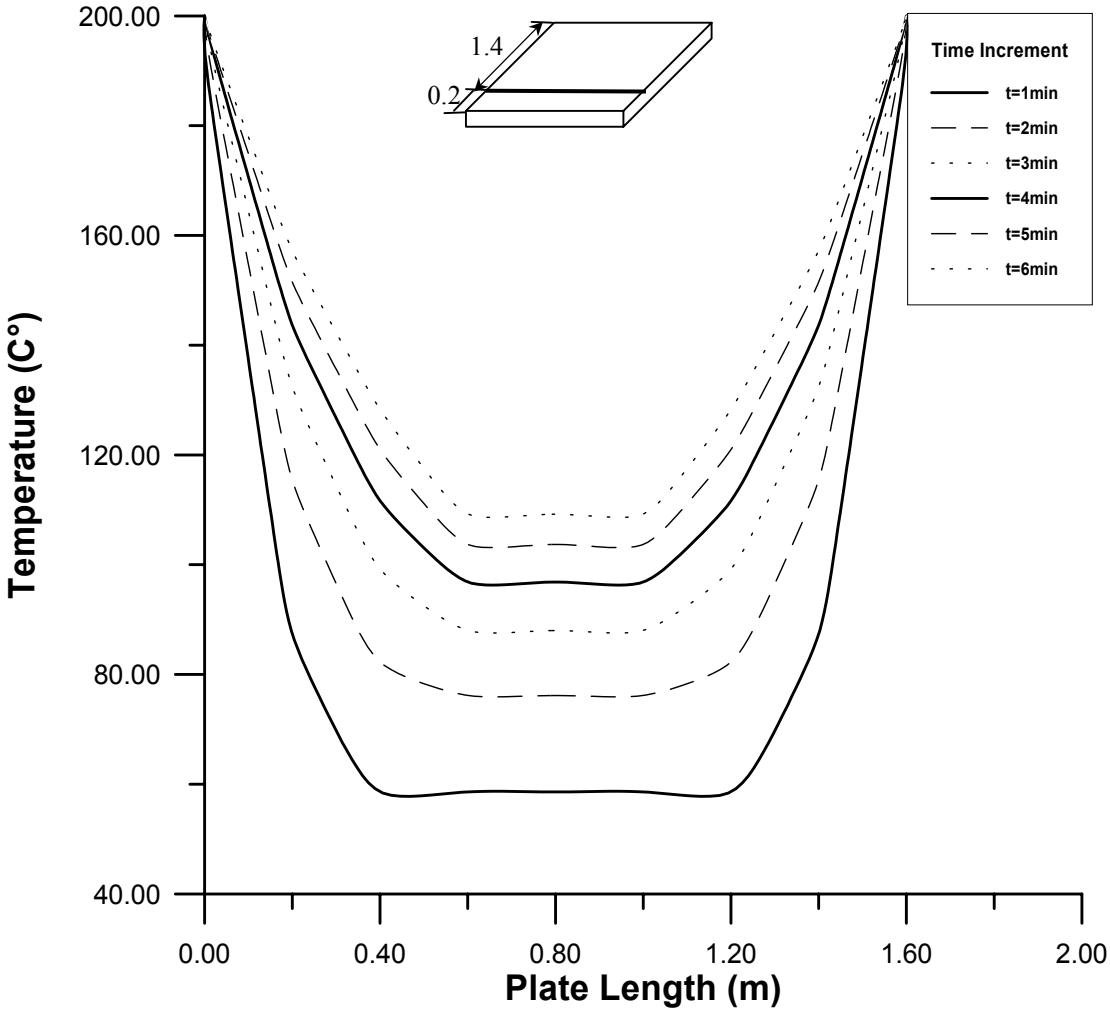

Figure 4-1: temperature against plate length in flat plate for k=386 W/m .C° at different time increment

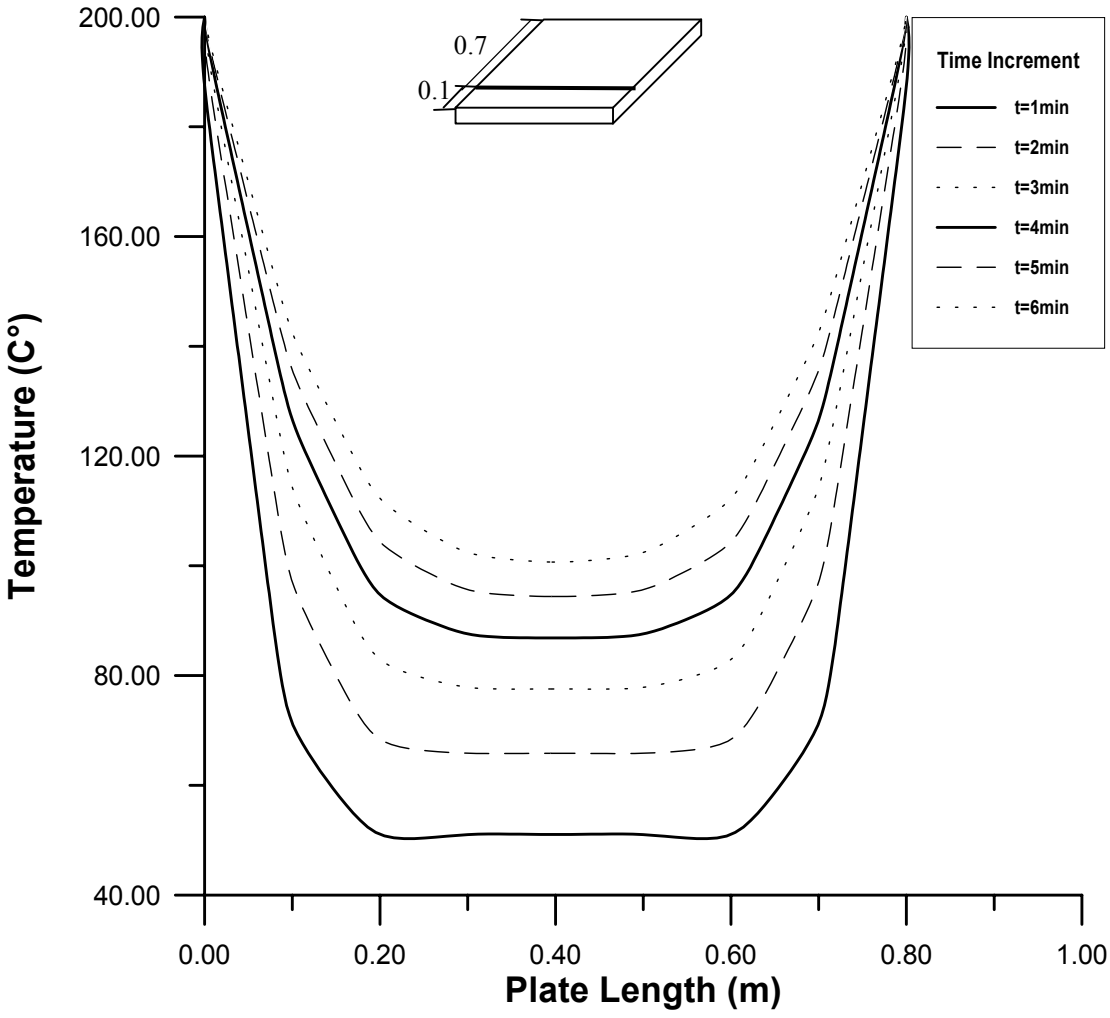

Figure 4-2: temperature against plate length in flat plate for k=73 W/m .C° at different time increment

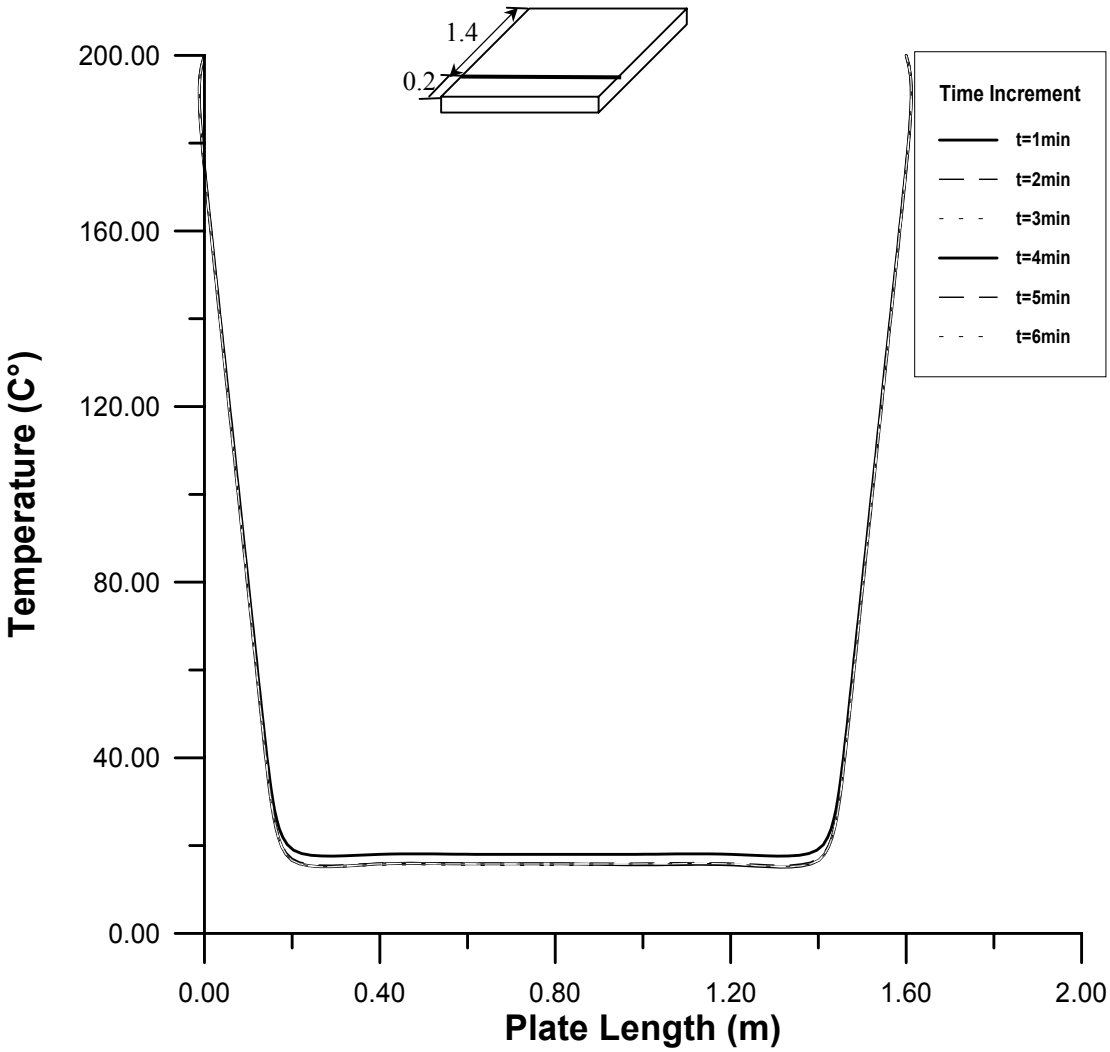

Figure 4-3: temperature against plate length in flat plate for k=0.038 W/m .C° at different time increment

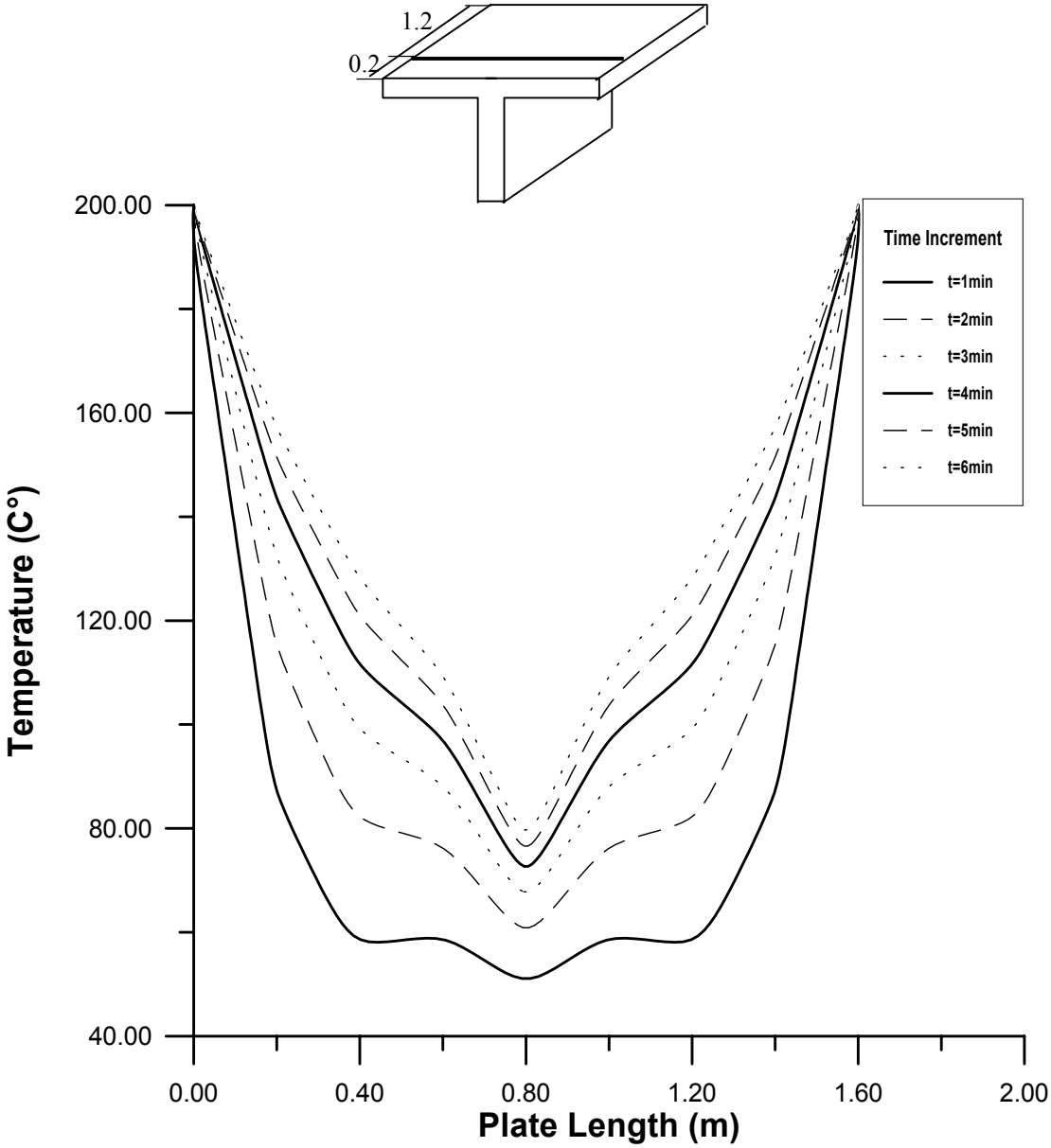

Figure 4-4: temperature against plate length in (T-element) for k=386W/m .C° at different time increment

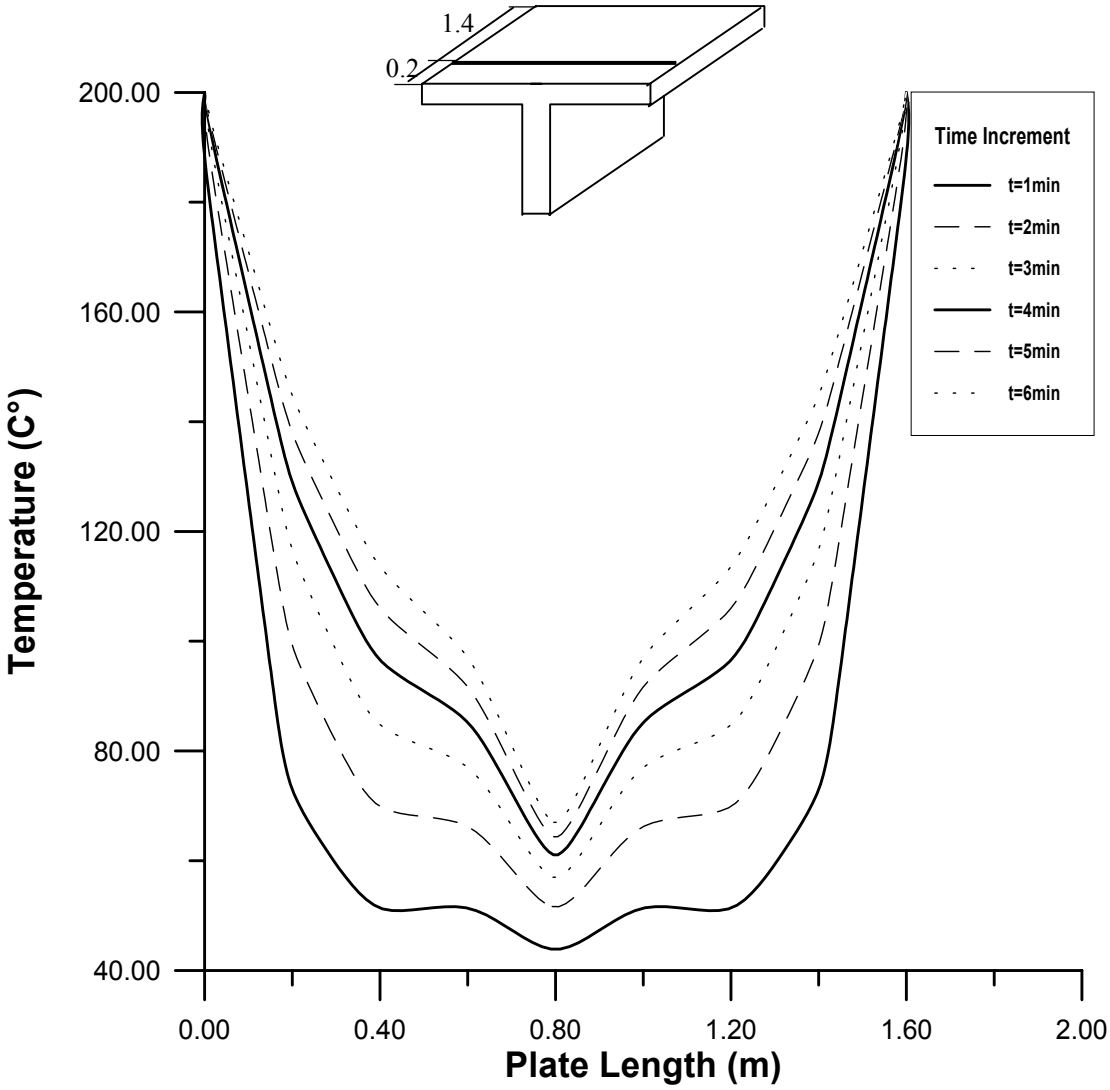

Figure 4-5: temperature against plate length in (T-element) for k=204W/m .C° at different time increment

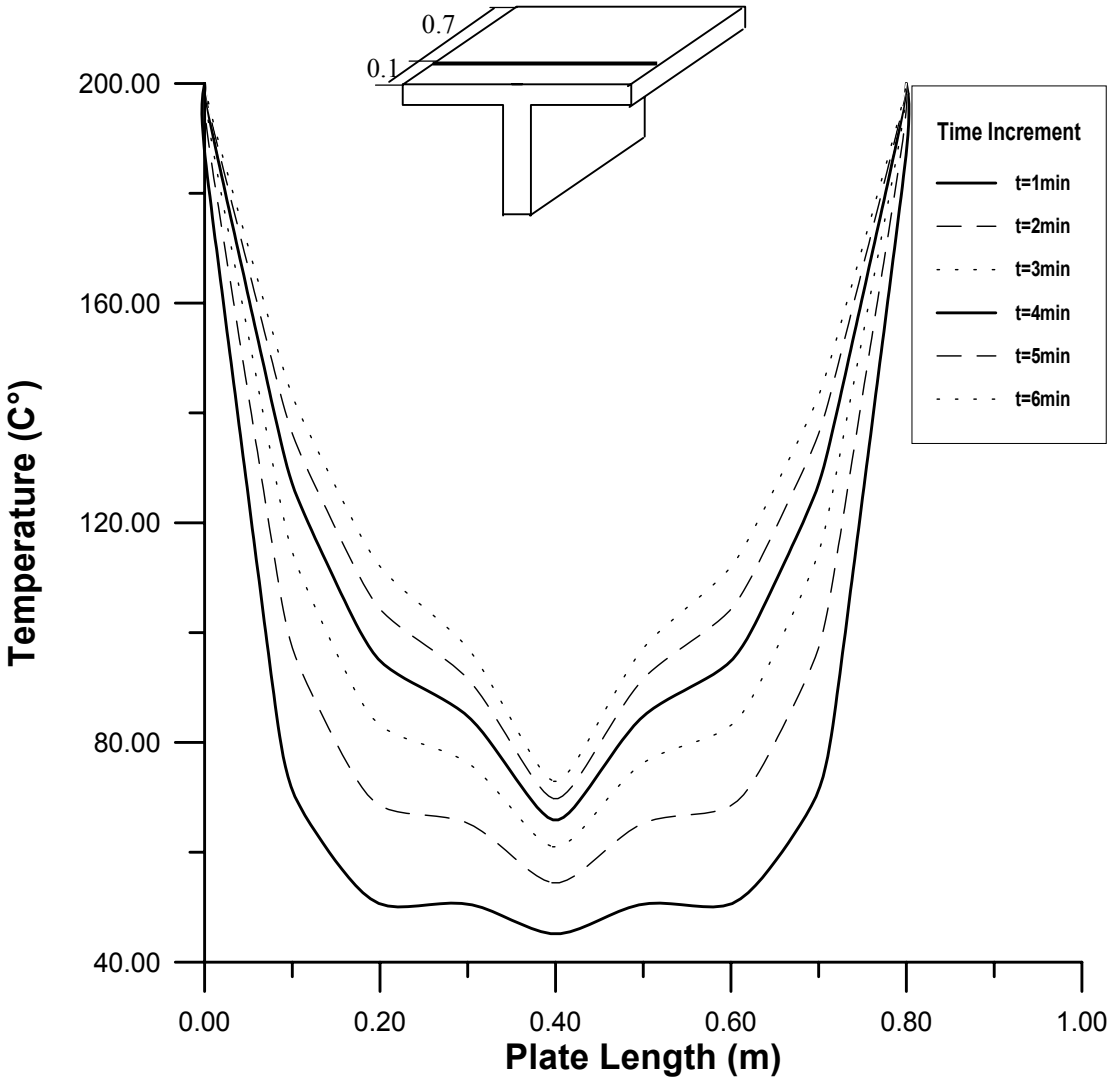

Figure 4-6: temperature against plate length in (T-element) for k=73W/m .C° at different time increment

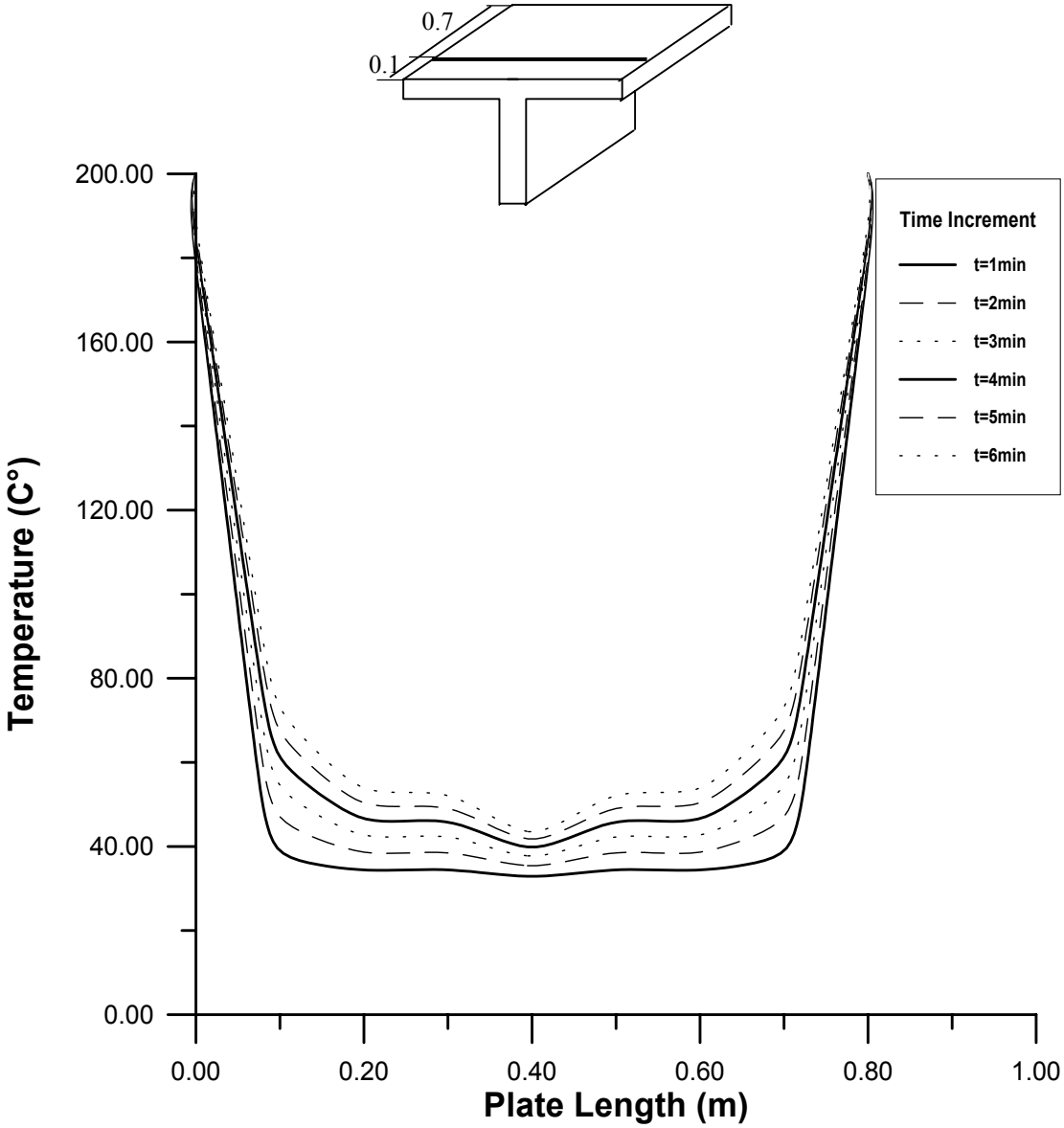

Figure 4-7: temperature against plate length in (T-element) for k=17W/m .C° at different time increment

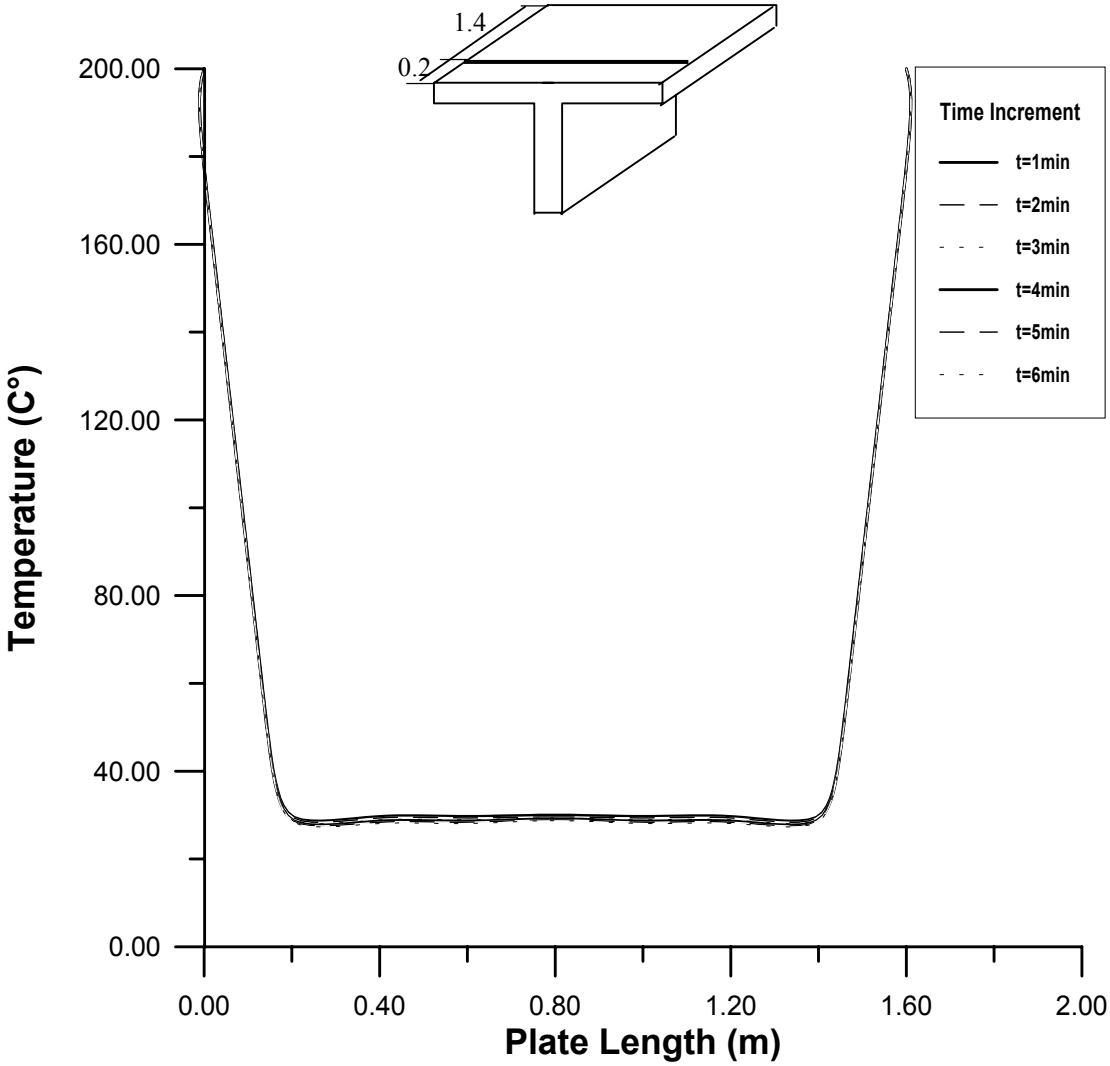

Figure 4-8: temperature against plate length in (T-element) for k=0.154W/m .C° at different time increment

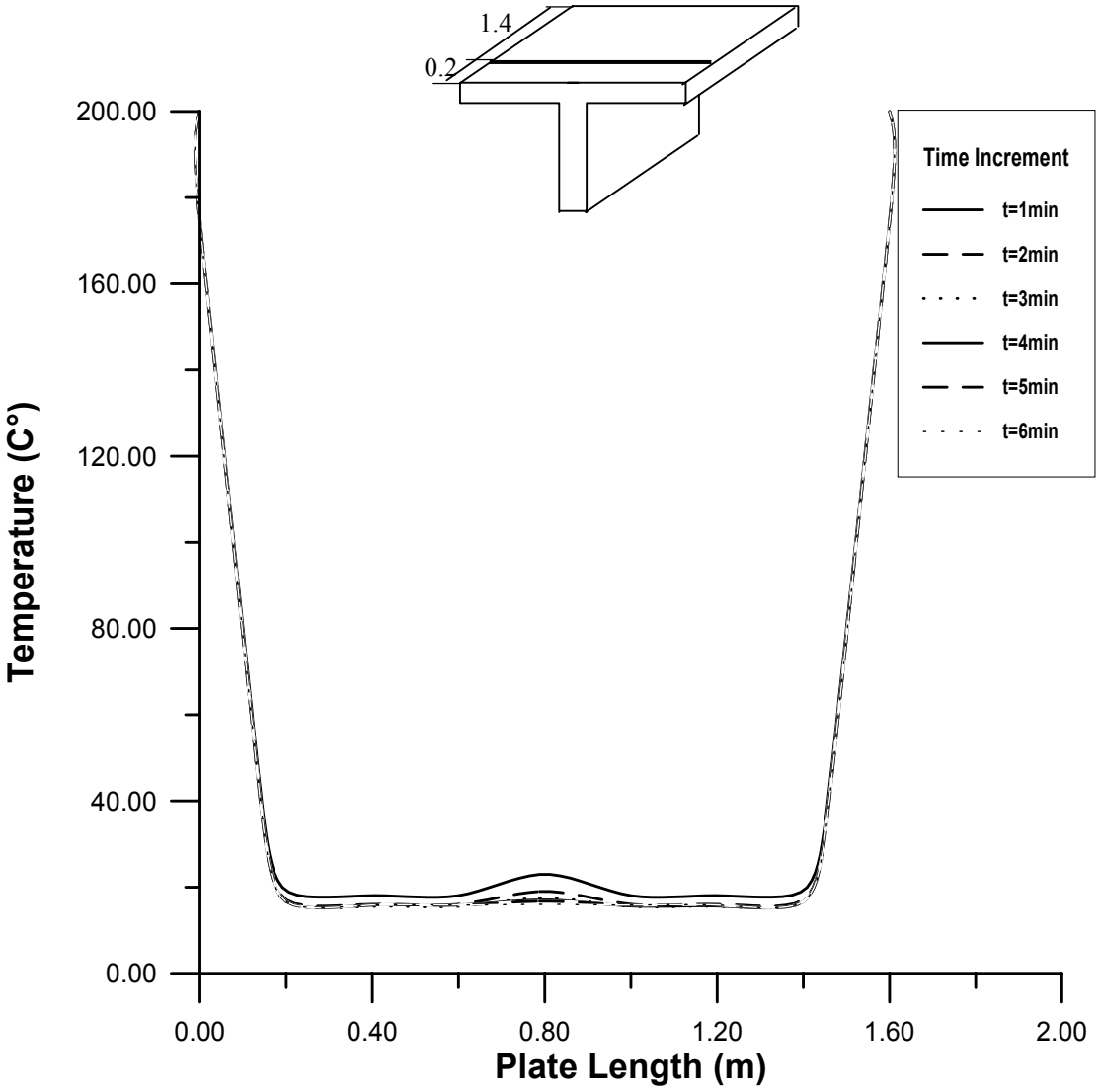

Figure 4-9: temperature against plate length in (T-element) for k=0.083W/m .C° at different time increment

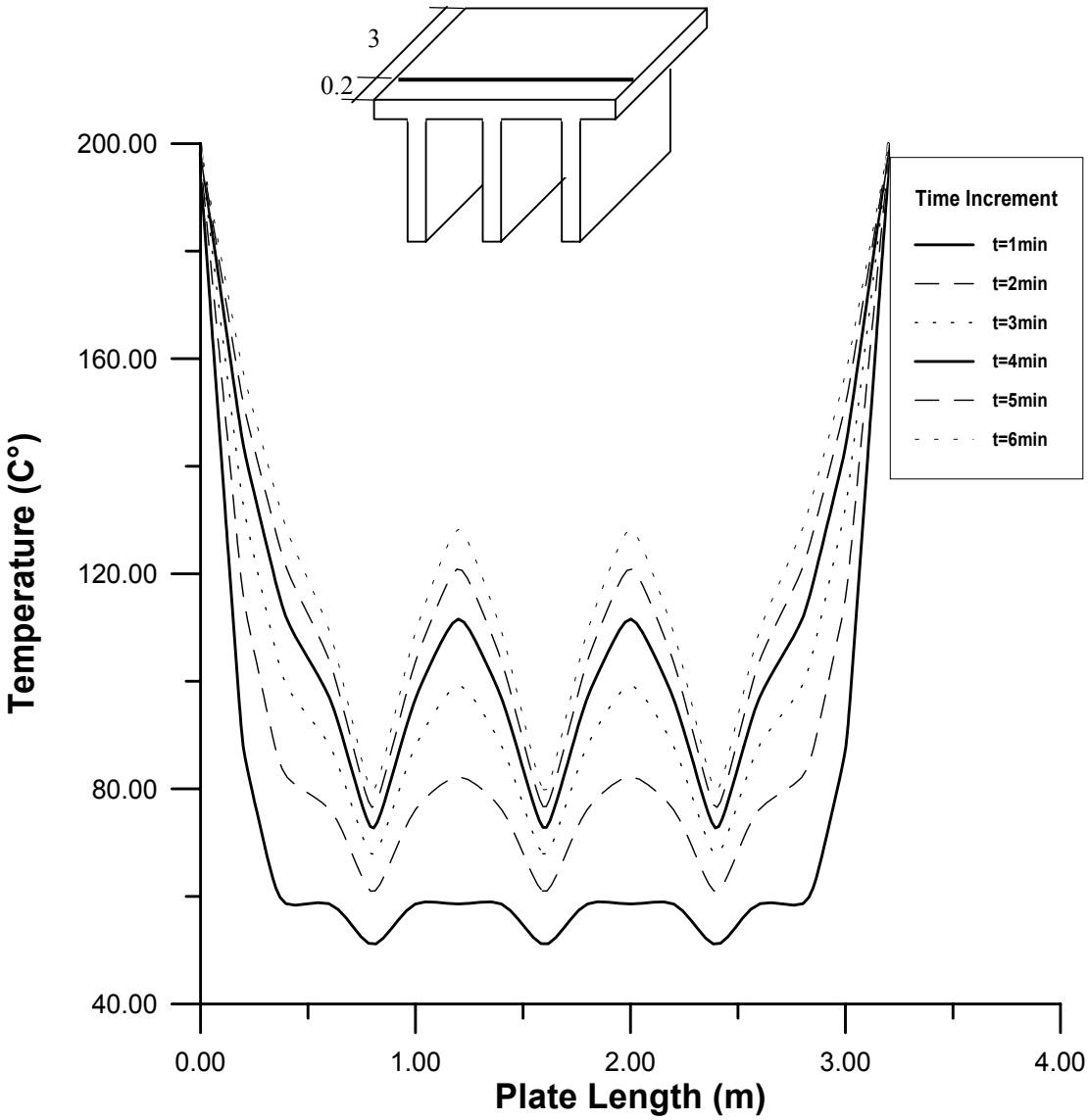

Figure 4-10: temperature against plate length in (stiffened structure plate) for k=386W/m .C° at different time increment

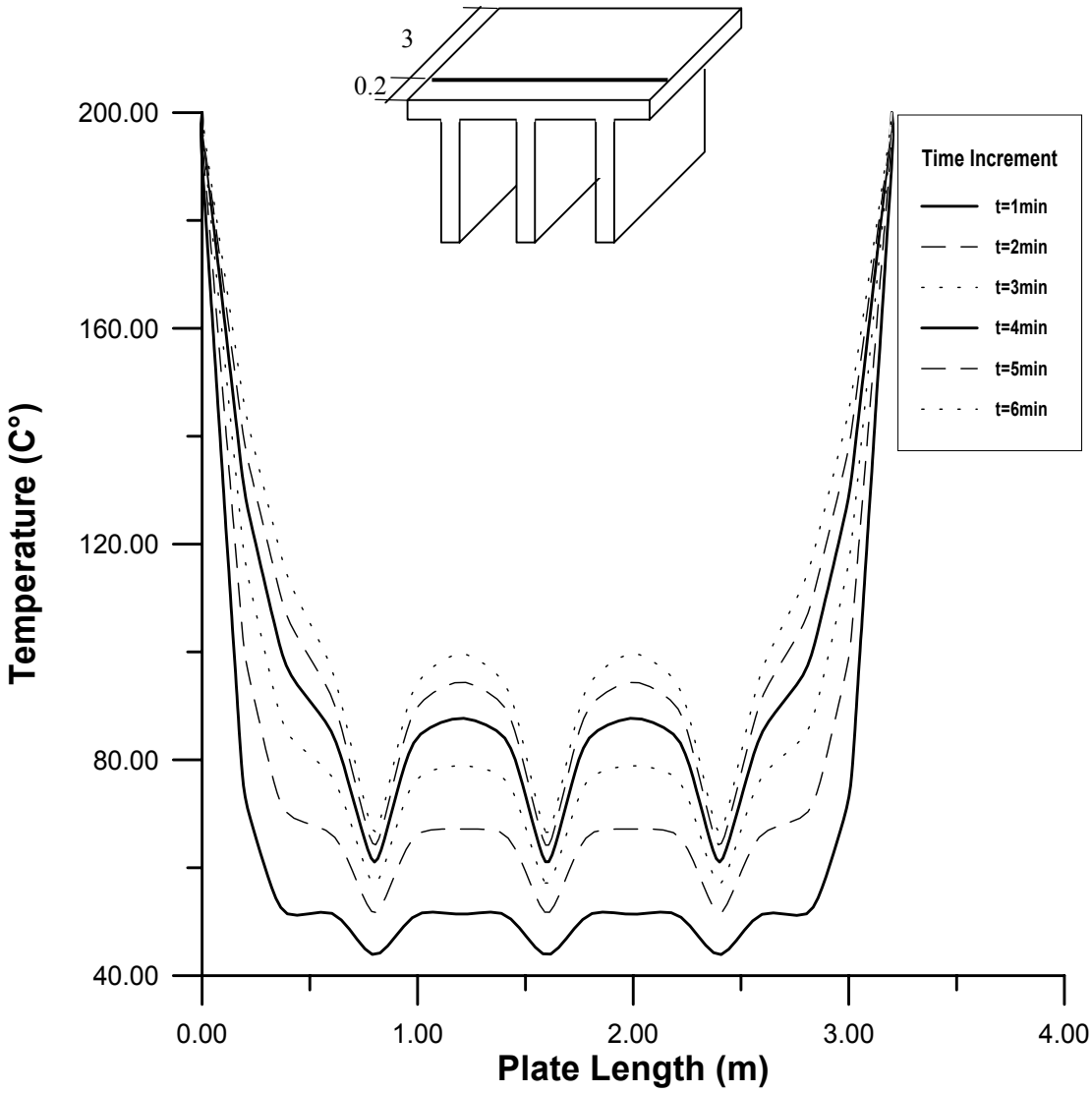

Figure 4-11: temperature against plate length in (stiffened structure plate) for k=204W/m .C° at different time increment

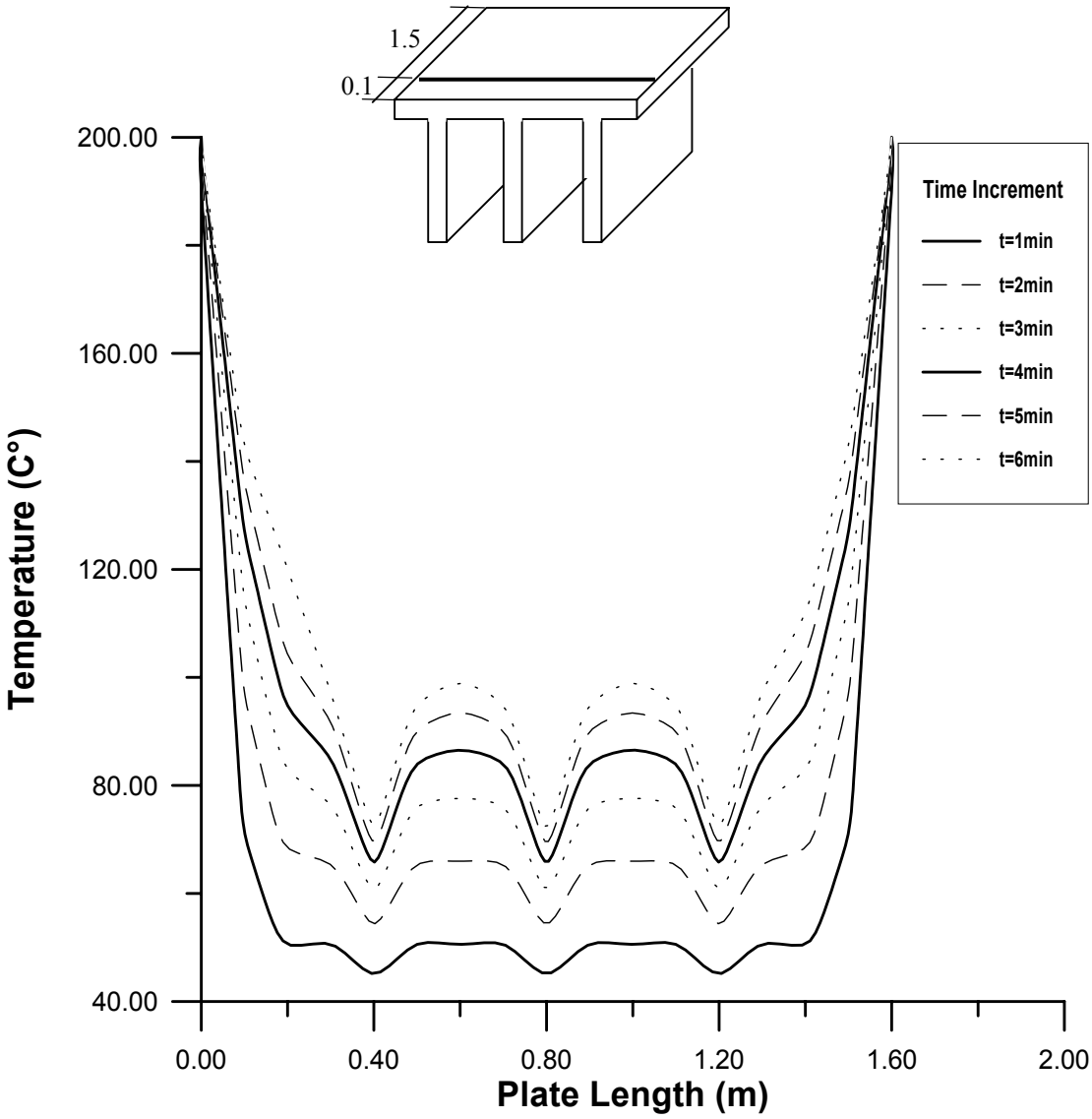

Figure 4-12: temperature against plate length in (stiffened structure plate) for k=73W/m .C° at different time increment

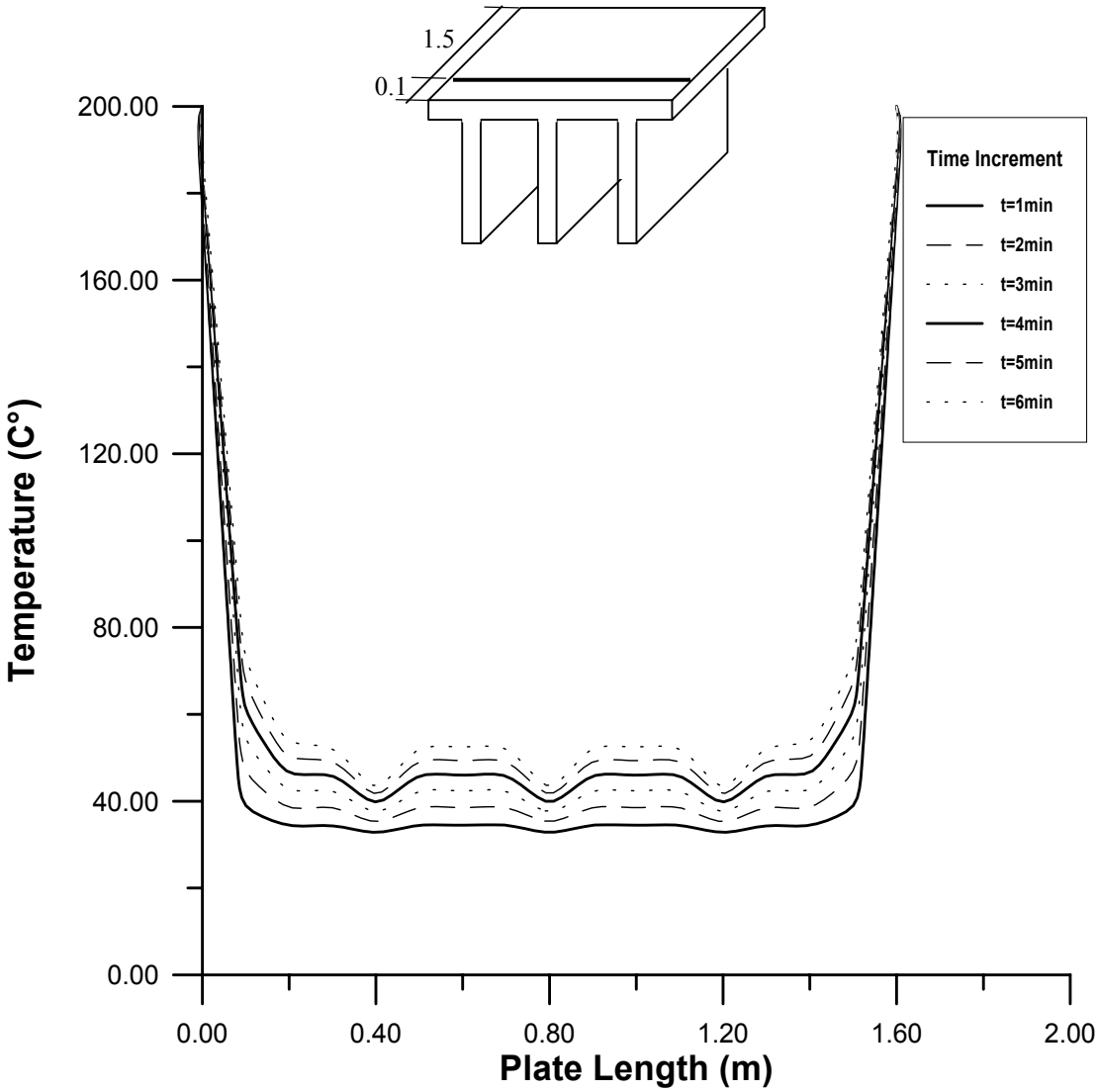

Figure 4-13: temperature against plate length in (stiffened structure plate) for k=17W/m .C° at different time increment

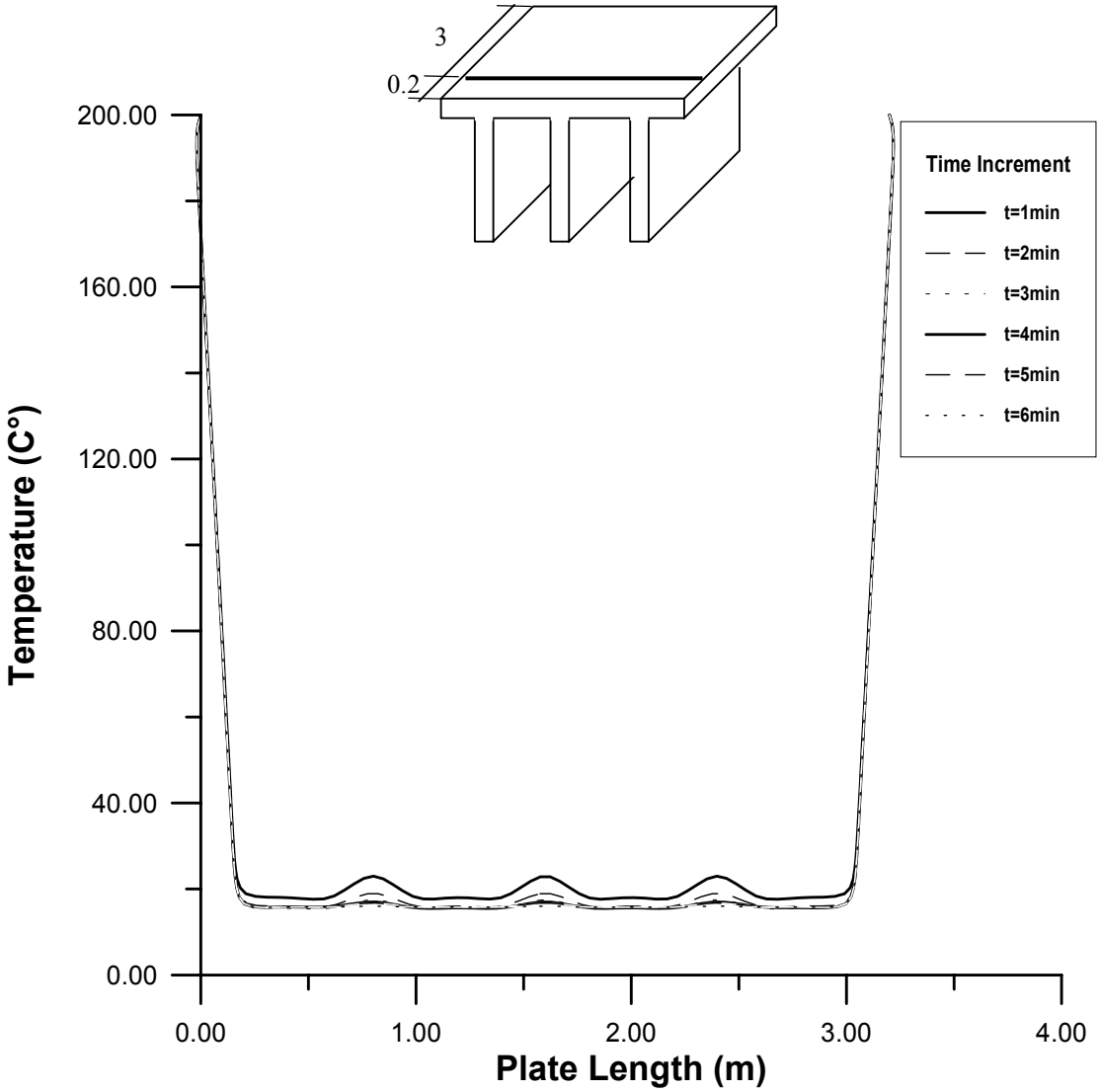

Figure 4-14: temperature against plate length in (stiffened structure plate) for k=0.038W/m .C° at different time increment

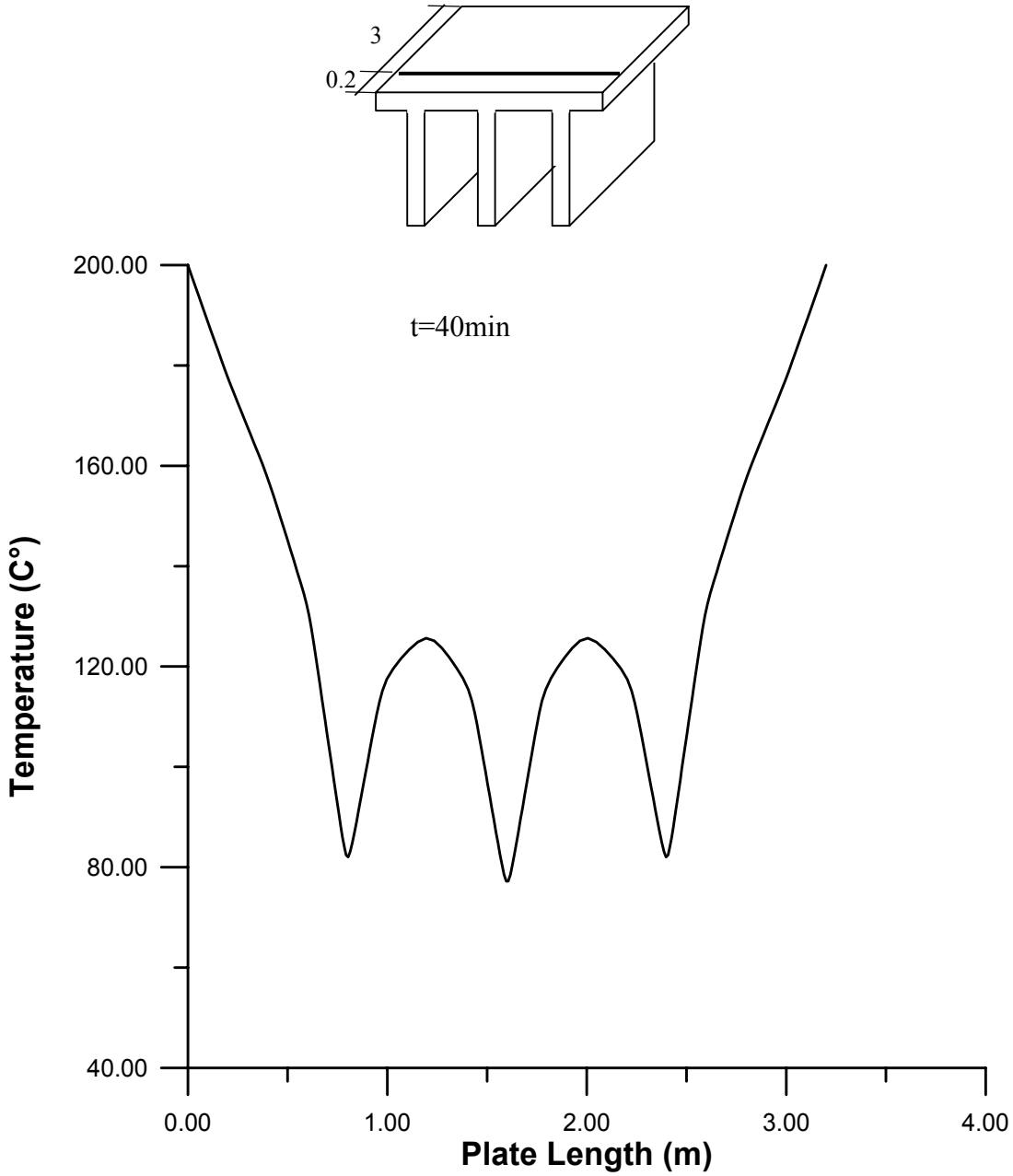

Figure 4-15: temperature against plate length in (stiffened structure plate) for k=204W/m .C° at t=40min

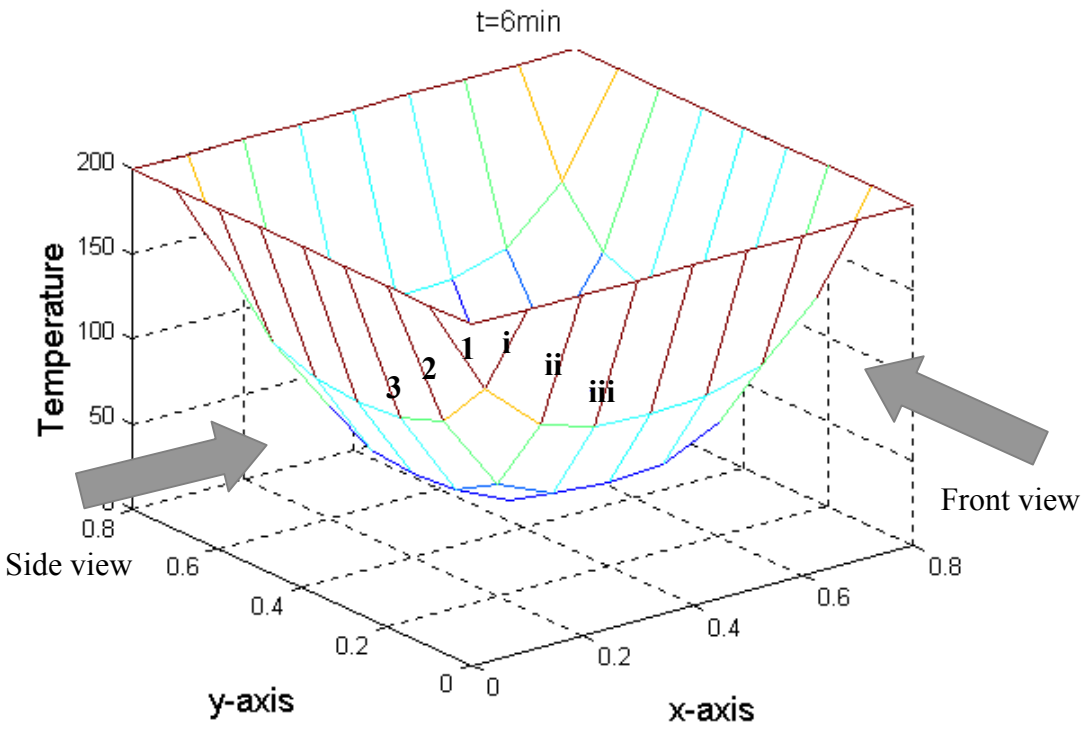

-a-

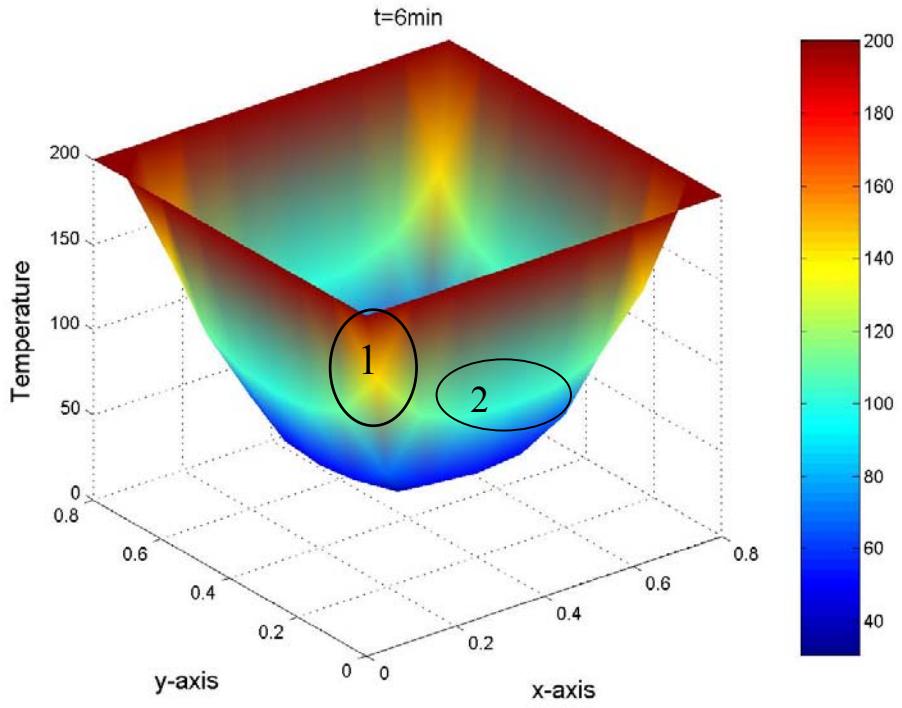

-b-

Figure 4-18: Contour presentation of temperature distribution in flat plate for k=73 W/m .C° at t=6min a-Mesh type, b= Color type

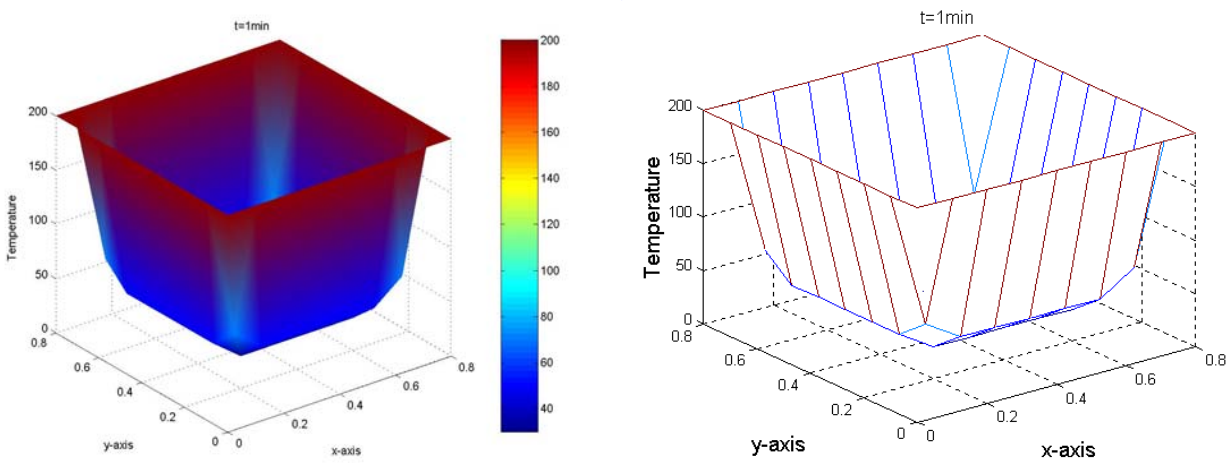

-a-

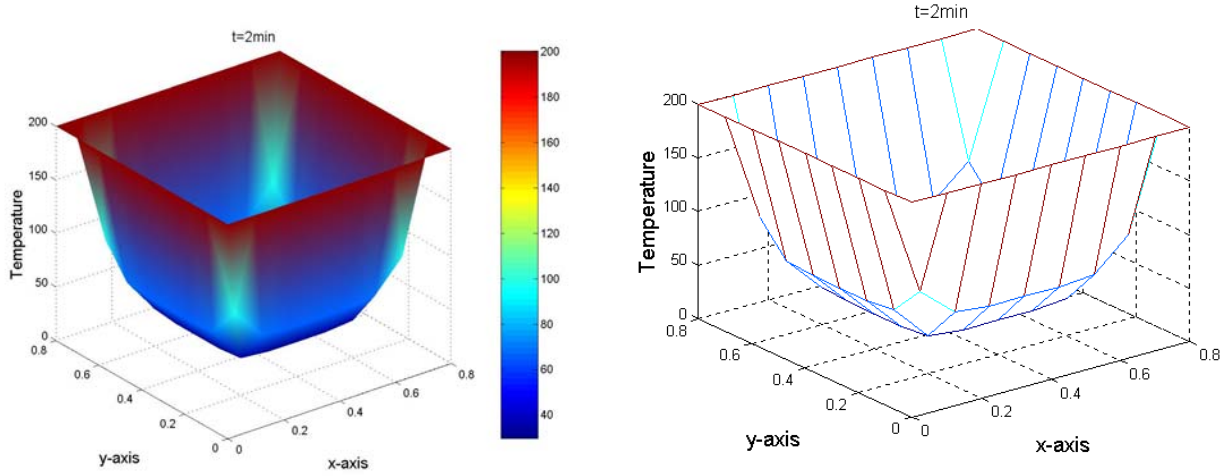

-b-

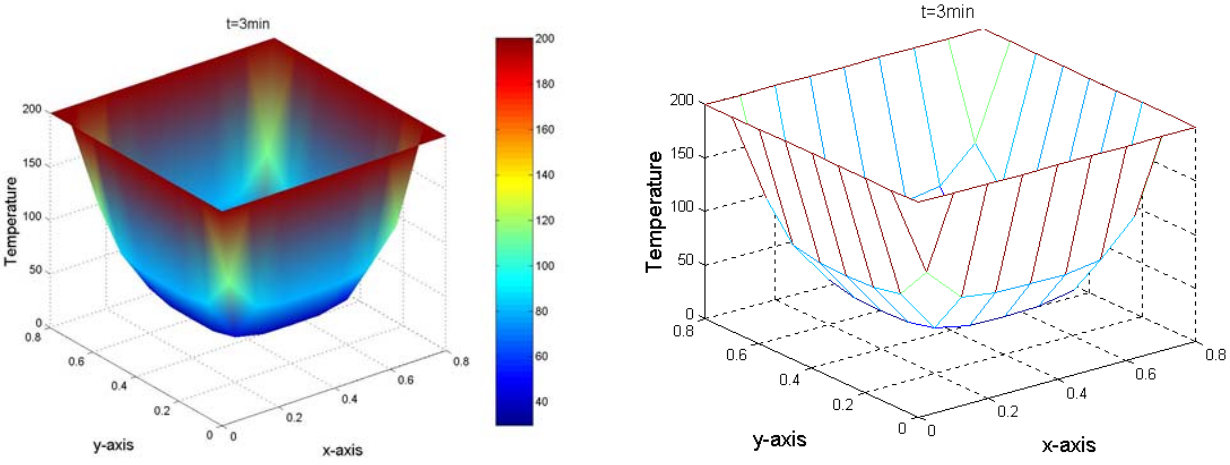

-c-

Figure 4-19: Contour presentation of temperature distribution in flat plate for k=73 W/m .C° at different time increment a, t=1min;b, t=2min;c, t=3min

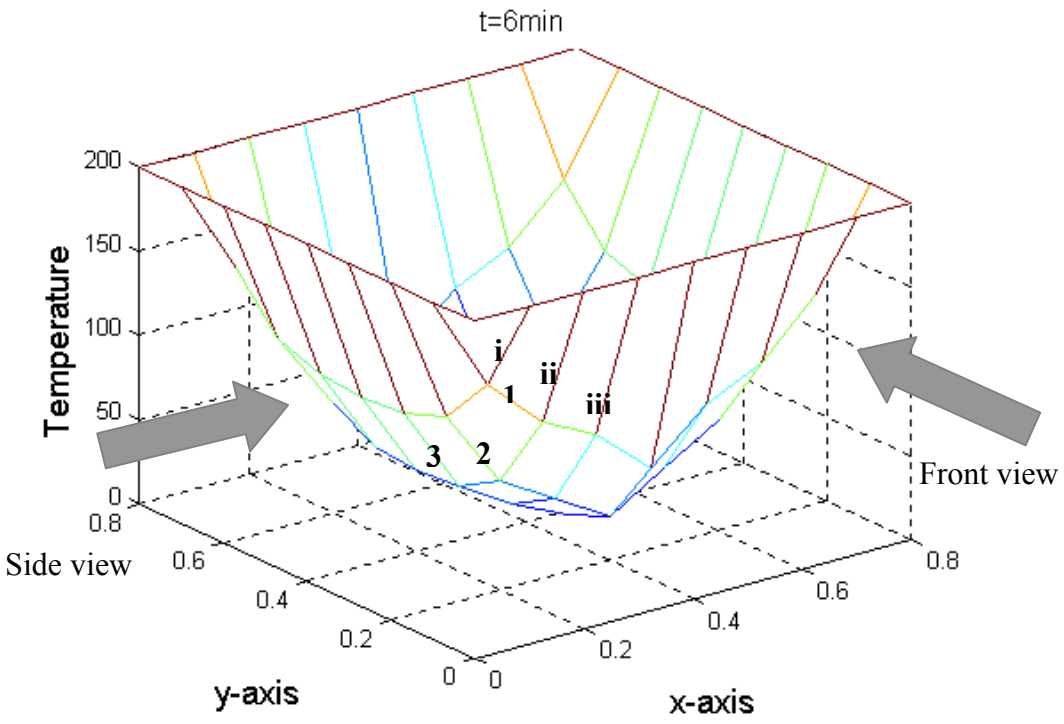

-a-

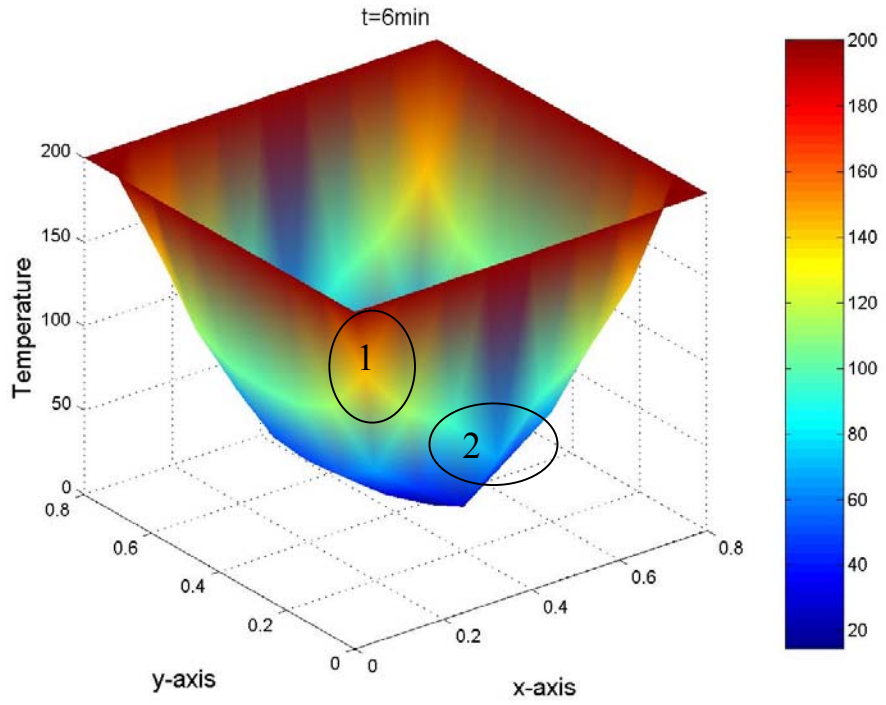

-b-

Figure 4-20: Contour presentation of temperature distribution in skin of T-element for k=73 W/m .C° at t=6min a-Mesh type; b= Color type

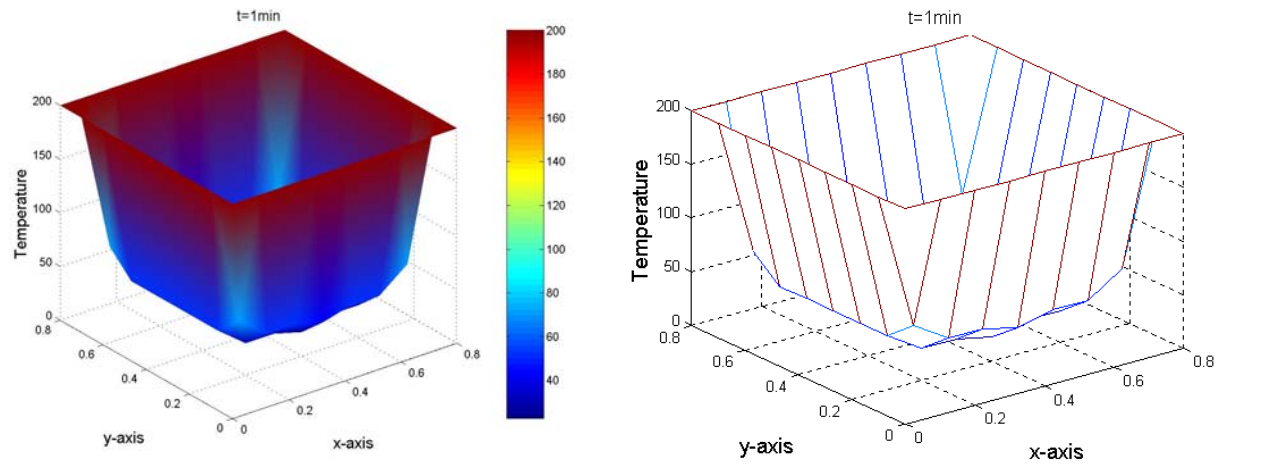

-a-

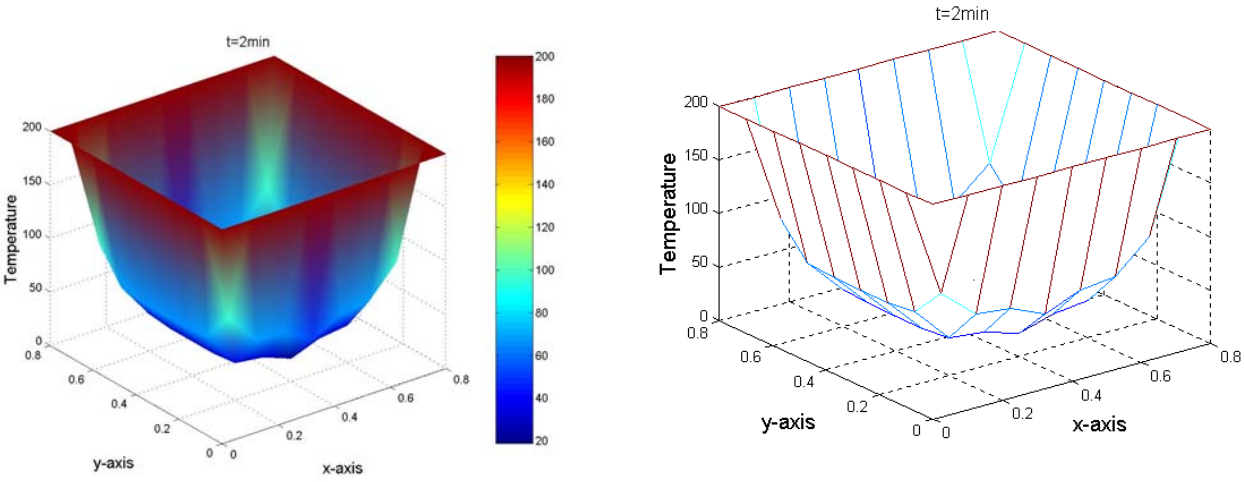

-b-

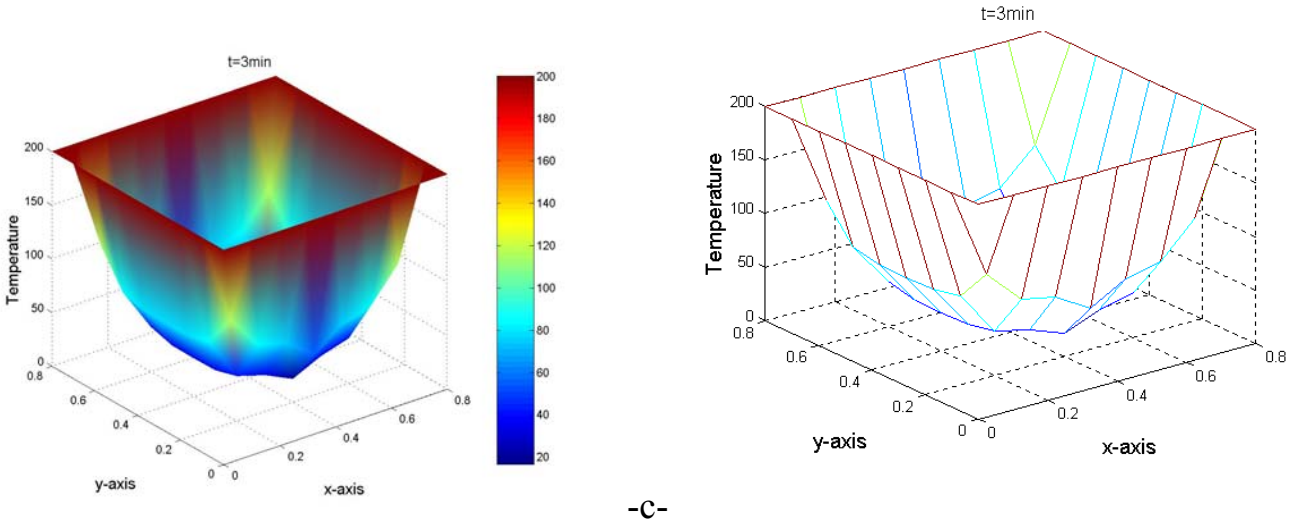

-c-

Figure 4-21: Contour presentation of temperature distribution in skin of T-element for k=73 W/m .C° at different time increment a, t=1min;b, t=2min;c, t=3min

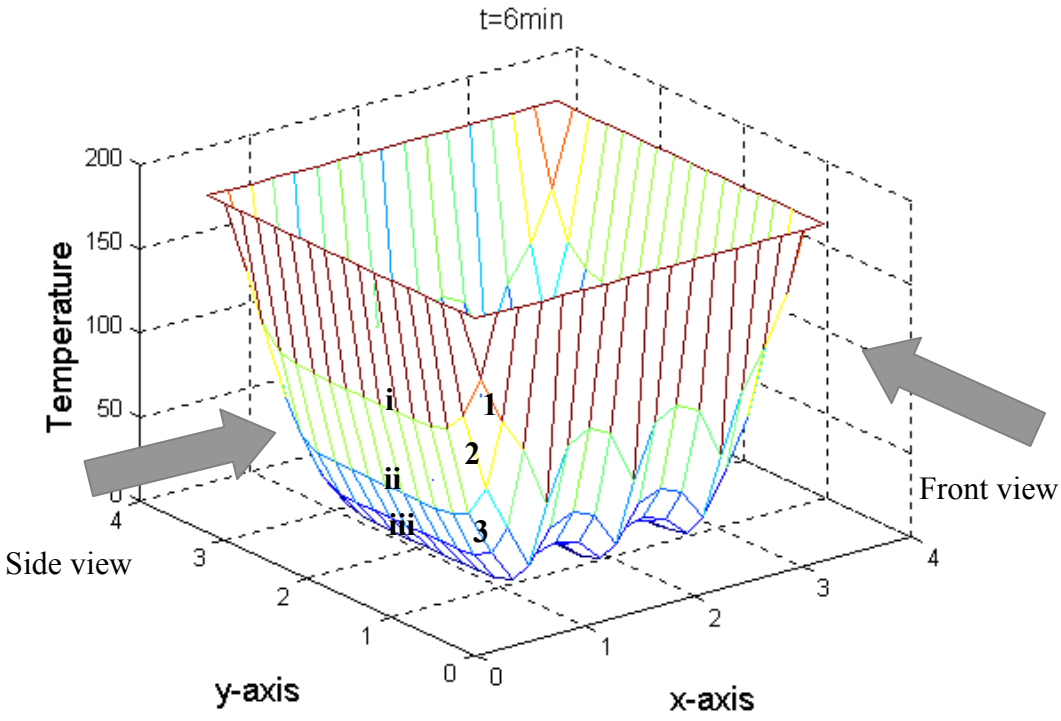

-a-

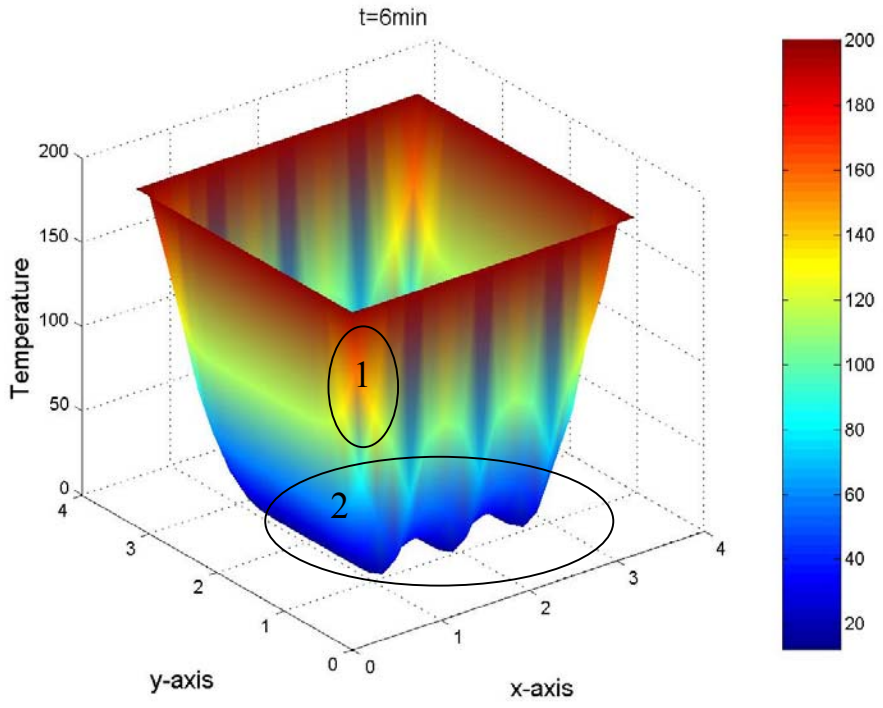

-b-

Figure 4-22: Contour presentation of temperature distribution in skin of stiffened structure plate for k=386 W/m .C° at t=6min a-Mesh type; b= Color type

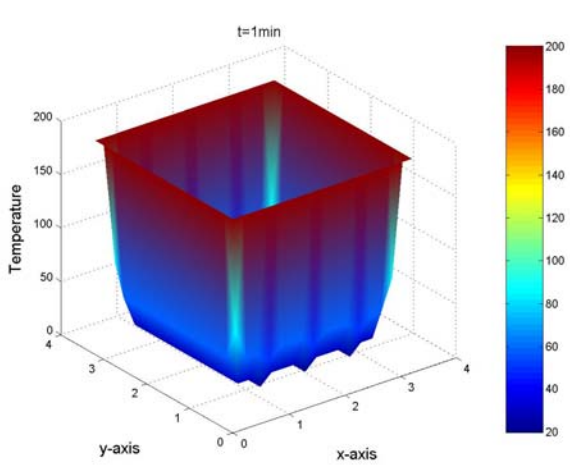

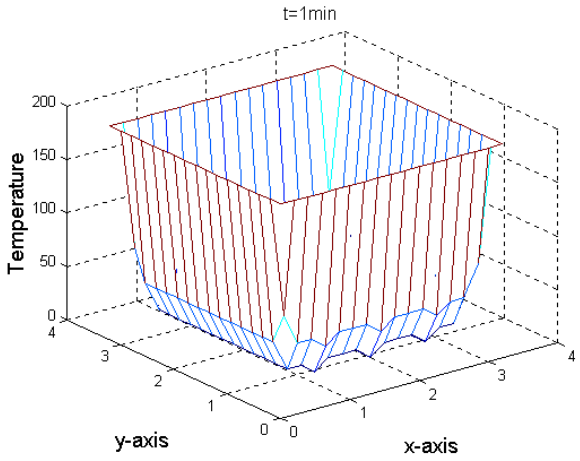

-a-

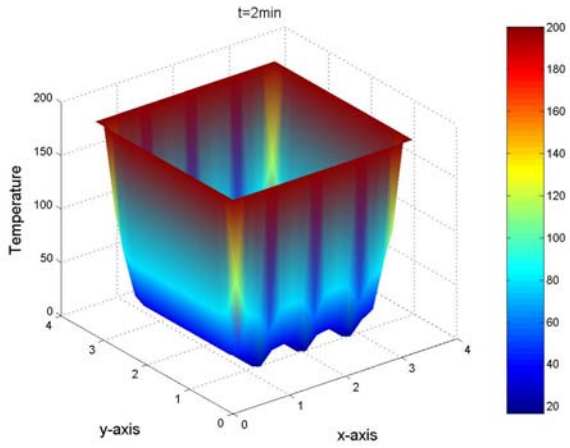

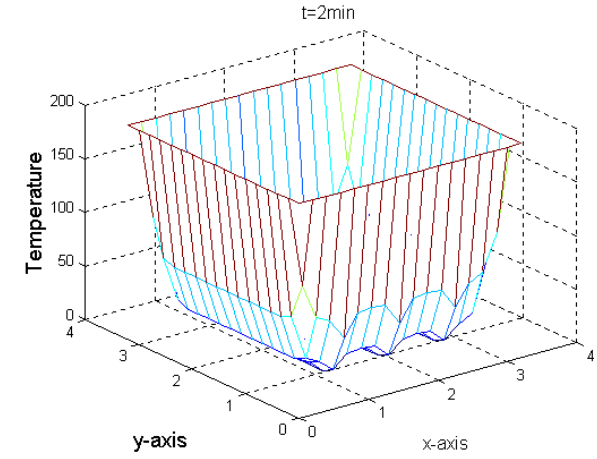

-b-

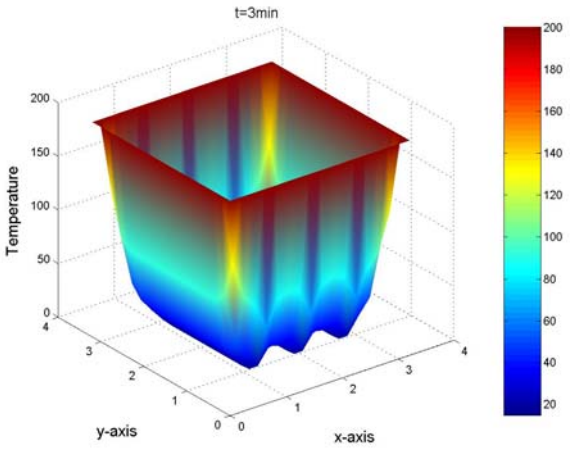

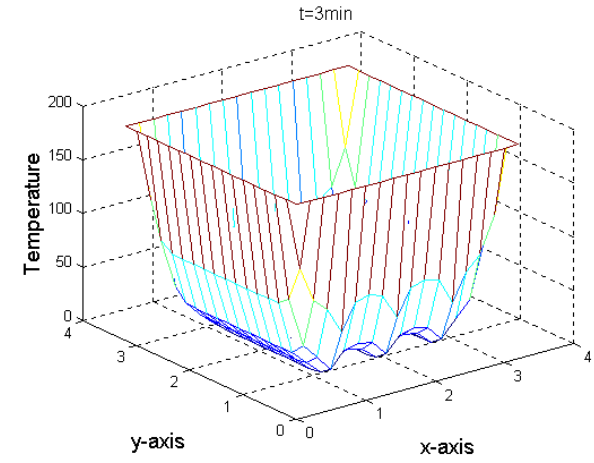

-c-

Figure 4-23: Contour presentation of temperature distribution in skin of stiffened structure for k=386 W/m .C° at different time increment a, t=1min;b, t=2min;c, t=3min

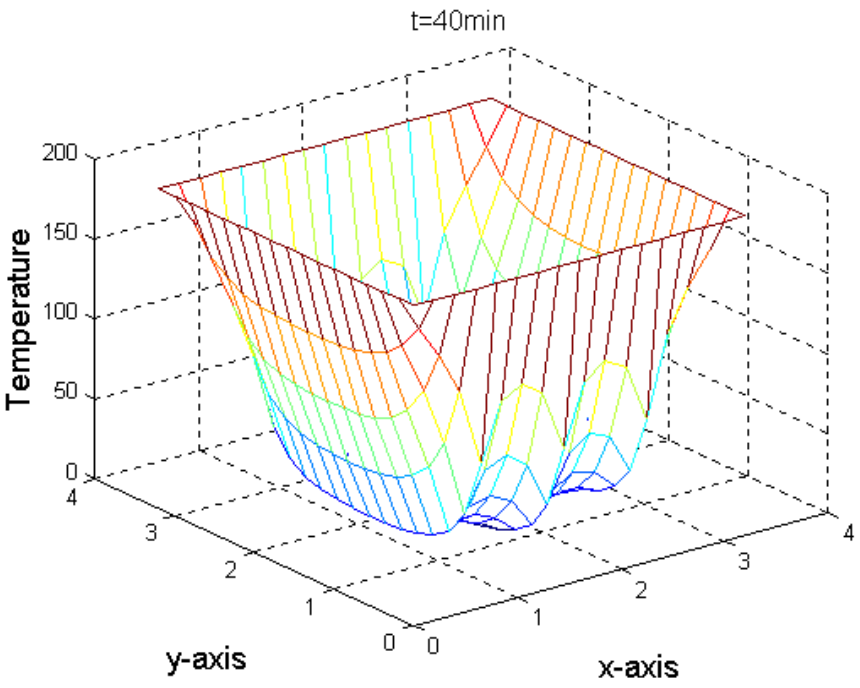

-a-

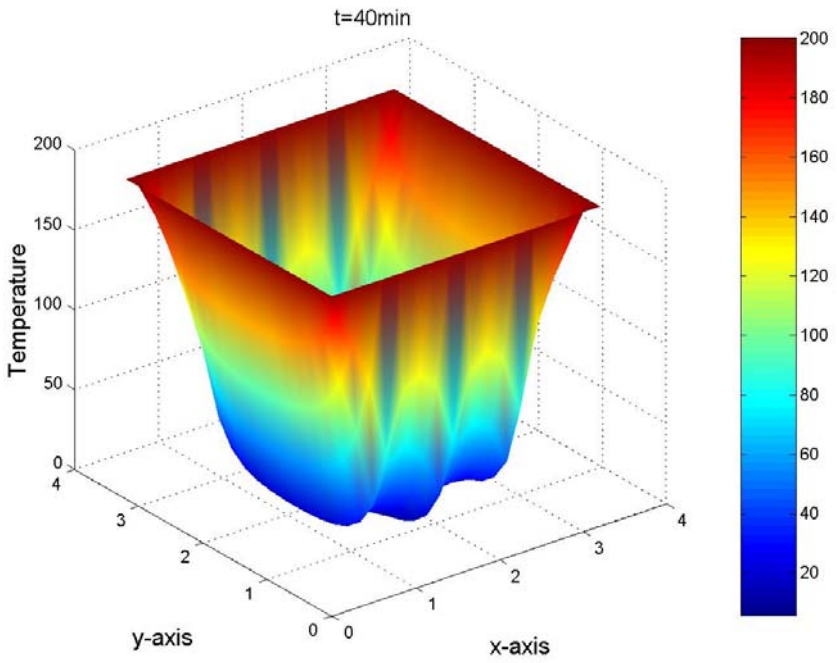

-b-

Figure 4-24: Contour presentation of temperature distribution in skin of stiffened structure plate for k=204 W/m .C°
at t=40min a-Mesh type; b=Color type

Chapter One

Introduction:

Heat transfer is energy in transit, which occurs as a result of a temperature gradient or difference. This temperature difference is thought of as a driving force that causes heat to flow. Heat transfer occurs by three basic mechanisms or modes: conduction, convection and radiation. Conduction is the transmission of heat through a substance without perceptible motion of the substance it self. Heat can conduct through gases, liquids and solids. Conduction is the transmission of heat in liquids is the same as for gases – random collisions of high – energy molecules with low – energy molecules causing a transfer of heat. The situation with liquids is more complex. However, because the molecules are more closely spaced. Therefore molecular force field can have an effect on the energy exchange between molecules; that is, molecular force field can influence the random motion of the molecules. Conduction of heat in solids is thought to be due to motion of free electrons, lattice waves, magnetic excitations, and electromagnetic radiation. The molecular energy of vibration in a substance is transmitted between adjacent molecules or atoms from a region of high to low temperature.

Convection is the term applied to heat transfer due to bulk movement of a fluid. Radiation is the transfer of energy by electromagnetic radiation having a defined range of wavelengths. Heat is usually transferred by a combination of conduction, convection, and radiation [1].

Many problems involving heat and mass transfer are reducible to the solution of partial differential equations. The differential equations that govern real physical processes are generally of a very complicated nature, and their closed- form is possible only in the simple cases.

Approximate methods therefore become very useful for the solution of such problems. The methods generally are divided into two categories. The first category covers those methods that allow an analytical expression. The second category of approximate methods is composed of numerical techniques that allow the determination of a table of approximate values of the desired solution. In this category are such approaches as the finite – difference method, straight-line method, large - particle method, and Monte Carlo method. The finite- difference technique is certainly the most universal and most widely used [2].

Thermal simulation play an important role in the design of many engineering applications, including internal combustion engines, turbines, heat exchangers, piping systems, and electronic components. In many cases engineers follow a thermal analysis with a stress analysis to calculate thermal stresses.

External surfaces of many of today's aircraft are designed with stiffened panels. Some various shaped stiffening members commonly used for panel structural concepts are shown in figure (1-1). The stiffening member provides the benefit of added load-carrying capability with a relatively small additional weight penalty [3].

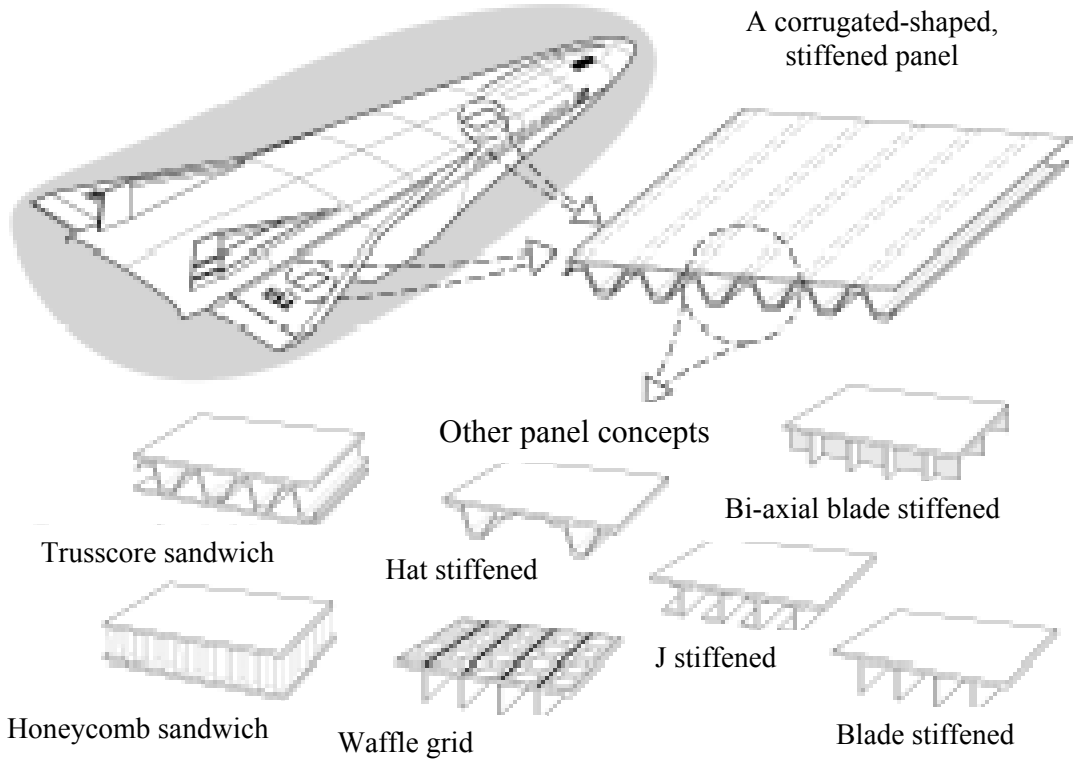

Figure 1-1: The Formulation can be applied to any stiffened, composite panel concept.

For the determination of transient temperature in geometrically sophisticated structures such as aero/space structure which are aerodynamically heated due to supersonic flight as shown in figure (1-2). The finite difference methods have to be applied. By increasing the complexity of the governing equation it is possible to predict the aero dynamical heating of structures such as re-entry vehicles or blades in a jet engine [4].

In industry fins are used in numerous applications, such as electrical equipment to help dissipate unwanted or potentially harmful heat.

Fins designed for cooling electronic equipment are shown in figure (1-3).

Another application of fins in single and double-pipe heat exchanger changer, as found in boiler and in radiator perhaps a more familiar

application of fins is found in air- cooled engine or compressors, where circumferential fins are integrally cast as part of a cylinder wall [5].

The purpose of adding extended surface is to help dissipate heat and if the temperature distribution is known, then the heat transfer rate can be determined.

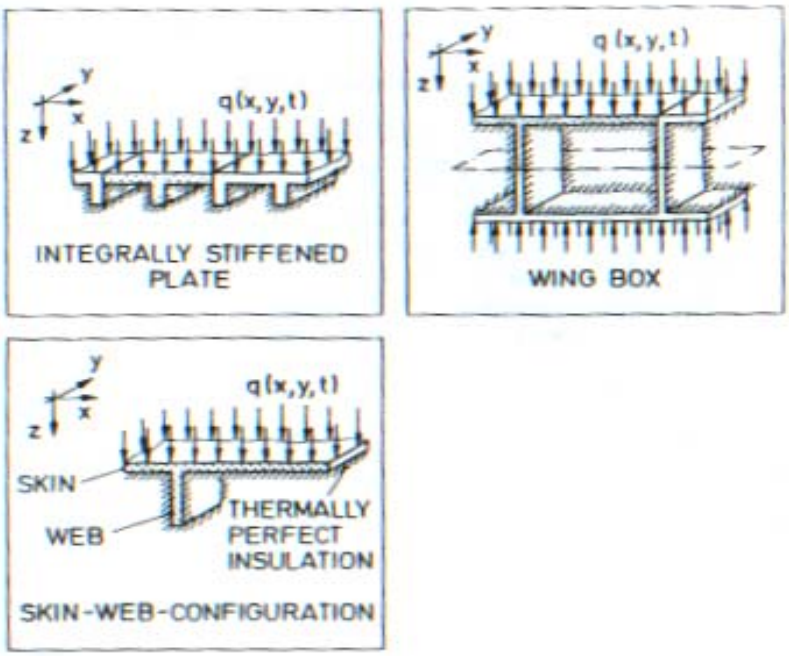

Figure 1-2: Typical aero/space structural elements

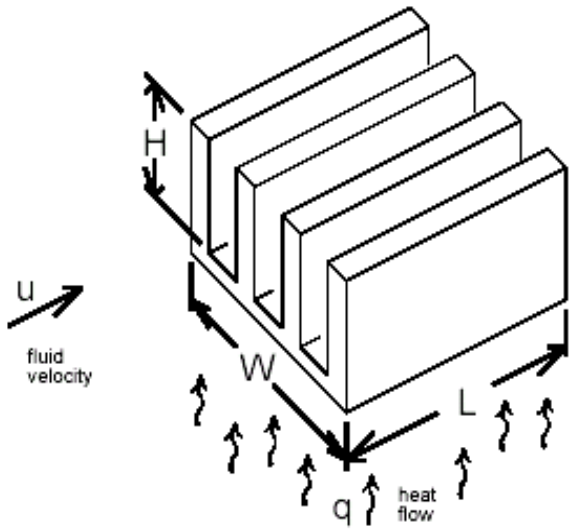

Figure 1-3: Heat sink

The Objectives of this work are to find the temperature distribution for different time interval on different structures numerically using transient finite difference method and study the effect of different value of thermal conductivity on the shape of temperature profile.

Chapter Three

Numerical Analysis

3.1: Numerical Method

There are many practical engineering problems for which exact solution cannot be obtained may be attributed to either the complex nature of governing differential equations or the difficulties that arise from dealing with the boundary and initial conditions, to deal with such problems, it resort to numerical approximations .In contrast to analytical solutions. Which show the exact behavior of a system at any point with in the system, numerical solutions approximate exact solutions only at discrete point, called nodes. The first step of any numerical procedure is discretization. This process divides the medium of interest into a number of small sub regions and nodes. There are two common classes of numerical methods [25]:

1- Finite difference method

2- Finite element method

In both approaches, the governing partial differential conduction equation subject to specified boundary (And for transient problems, initial) conditions is transformed into a system of ordinary differential equations (for transient problems) or algebraic equations (for steady-state problems) Which are solved to yield an approximate solution for the temperature distribution. In the finite difference method, spatial discretization of the problem using a set of nodal points followed by application of energy balances and rate equations for each of the discrete segments directly results in a system of equations which are solved to obtain the temperature at each nodal point.

The use of finite difference methods is more transition between analytical methods and finite element. The main advantage of the finite difference method is that the it is rather simple and easily understandable physically (the variable are: temperature, time and spatial coordinates: in contrast to some mathematical functional in finite element analysis solution).

But with this method approximation of curvilinear areas is quite complicated. Inanition the FD method use uniform steps over the space – coordinate (it is possible to avoid this but it also severely complicates the task).

3.2: Finite Difference Method In Steady-State Heat Transfer By Conduction

In a large number of practical problems involving steady-state heat transfer in a solid conduction region, an exact mathematical solution is precluded as a result of the complex shape of the conduction region, the type of boundary condition, the energy generation rate per unit volume, variable thermal conductivity, or any combination of these.

In such situation, the temperature distribution can frequently be determined by an approximate finite difference analysis and partial differential equation.

The finite difference equation approximates the governing partial differential equation at a finite number of points within the conduction region, called nodes or nodal points, grid points by an algebraic finite difference equation at each point. Thus if (n) nodal points are selected at which a solution for the approximate steady-state temperature is desired (n) simultaneous algebraic equations for the (n) unknown temperatures are solved.

The main task of the engineer, when using finite difference methods, is the setting up, or derivation, of the algebraic finite difference equations, which are appropriate for the problem at hand [1].

3.3: Finite Difference Method In Unsteady-State Heat Transfer by Conduction

When the temperature at any point with in a conduction region is changing with time, the temperature distribution is termed (unsteady-state); that is an unsteady-state condition prevails.

The general unsteady-state conduction requires the determination of the temperature distribution in a solid conduction region as a function of space coordinates and the time.

The transient finite difference equation at any node of interest is arrived in a manner similar to that for the steady-state finite difference equation; that by making an energy balance on the volume of material associated with each node, leading to a set of algebraic equation for the (n) nodal temperatures that are to be solved at a finite number of times. At this point, the similarity between the steady-state finite difference equation and the transient finite difference equation often ends because of differences in the way the equation set is solved and the appearance of a phenomenon called the stability of the equation set [1].

3.4: Derivation of The General Heat – Conduction Equation

Consider the three-dimensional system shown in figure 3-1.

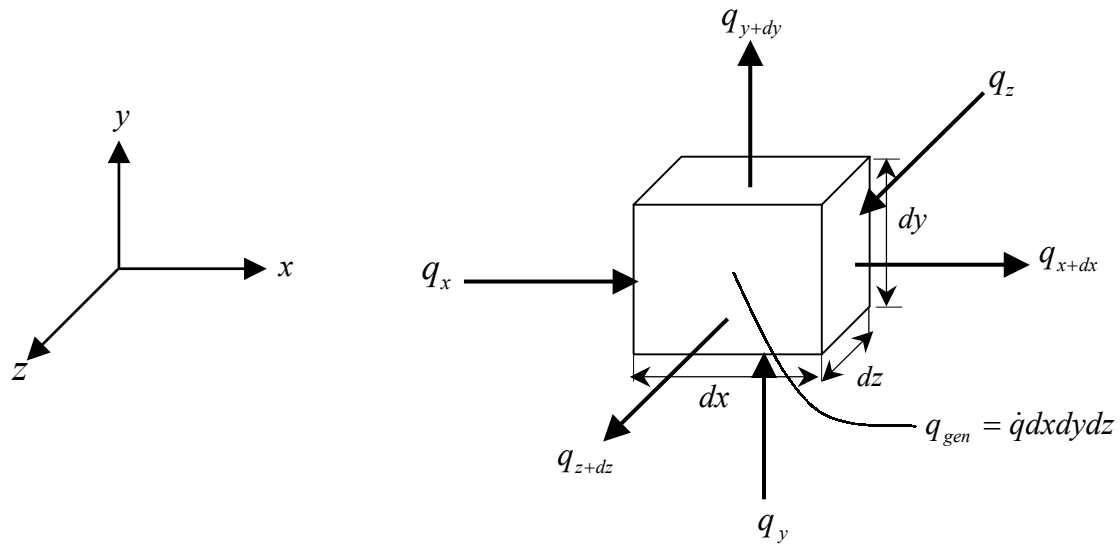

Figure 3-1: elemental volume for the three –dimensional heat conduction analysis (Cartesian coordinates)

The temperature distribution existing within a material can at most depends on three space variables and on time.

In this analysis the thermal conductivity is assumed to be constant and the variable is isotropic [26].

Make an energy balance on a control volume.

$$\begin{pmatrix} Rateofenergy \\ conducted\ \text{int}\ o \\ controlvolume \end{pmatrix} + \begin{pmatrix} Rateofenergy \\ Generatedinside \\ controlvolume \end{pmatrix} = \begin{pmatrix} Rateofenergy \\ conductedoutof \\ controlvolume \end{pmatrix} + \begin{pmatrix} Rateofenergy \\ stored \\ Insidecontrolvolume \end{pmatrix}$$

$$q_x + q_y + q_z + q_{gen} = q_{x+dx} + q_{y+dy} + q_{z+dz} + \frac{dE}{dt} \qquad (3\text{-}1)$$

And the energy quantities are given by:

Since $q = -KA\dfrac{dT}{dx}$

$\therefore\ q_x = -Kdydz\ \dfrac{\partial T}{\partial x}$

$$q_{x+dx} = q_x + \frac{\partial}{\partial x} q_x dx$$

$$= -\left[K \frac{\partial T}{\partial x} + \frac{\partial}{\partial x}\left(K \frac{\partial T}{\partial x} \right) dx \right] dy\, dz$$

$$q_y = -K\, dx\, dz \frac{\partial T}{\partial y}$$

$$q_{y+dy} = -\left[K \frac{\partial T}{\partial y} + \frac{\partial}{\partial y}\left(K \frac{\partial T}{\partial y} \right) dy \right] dx\, dz$$

$$q_z = -K\, dx\, dy \frac{\partial T}{\partial z}$$

$$q_{z+dz} = -\left[K \frac{\partial T}{\partial z} + \frac{\partial}{\partial z}\left(K \frac{\partial T}{\partial z} \right) dz \right] dx\, dy$$

$$q_{gen} = q^{\cdot}\, dxdydz$$

$$\frac{dE}{dt} = \rho\, c\, dx\, dy\, dz \frac{\partial T}{\partial t}$$

Substitute all these quantities into equation (3-1)

$$\frac{\partial}{\partial x}\left(K \frac{\partial T}{\partial x} \right) + \frac{\partial}{\partial y}\left(K \frac{\partial T}{\partial y} \right) + \frac{\partial}{\partial z}\left(K \frac{\partial T}{\partial z} \right) + q^{\cdot} = \rho\, c \frac{\partial T}{\partial t} \qquad (3\text{-}2)$$

For constant thermal conductivity Equation (3-2) is written

$$\frac{\partial^2 T}{\partial x^2} + \frac{\partial^2 T}{\partial y^2} + \frac{\partial^2 T}{\partial z^2} + \frac{q^{\cdot}}{K} = \frac{1}{\alpha} \frac{\partial T}{\partial t} \qquad (3\text{-}3)$$

Where $\alpha = \dfrac{K}{\rho c}$

In our problem since there is no heat generation and constant thermal conductivity. Equation (3-3) will be

$$\frac{\partial^2 T}{\partial x^2} + \frac{\partial^2 T}{\partial y^2} + \frac{\partial^2 T}{\partial z^2} = \frac{1}{\alpha} \frac{\partial T}{\partial t} \qquad (3\text{-}3a)$$

Two-dimensional problem (i.e. $\frac{\partial^2 T}{\partial z^2}$) and equation (3-3a) will be

$$\frac{\partial^2 T}{\partial x^2}+\frac{\partial^2 T}{\partial y^2}=\frac{1}{\alpha}\frac{\partial T}{\partial t} \tag{3-3b}$$

3.5: The Finite Difference Approximation of Derivative

Using Taylor's expansion method with reminder it can [27]

$$\phi(x_{l+1})=\phi(x_l+\Delta x)=\phi(x_l)+\Delta x\frac{d\phi}{dx}\Big|_{x=x_l}+\frac{\Delta x^2}{2}\frac{d^2\phi}{dx^2}\Big|_{x=x_l+\theta\Delta x} \tag{3-4}$$

Where (θ_l) is some in the range $0\le\theta_l\le 1$ using the subscript (l) Denote an evaluation at $x=x_l$ this can be written

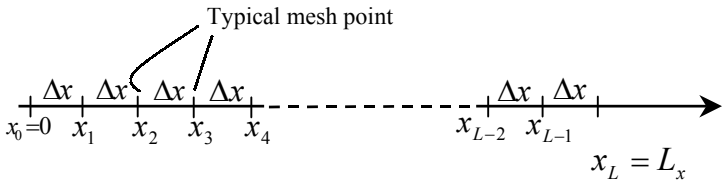

Figure 3-2: construction of a finite difference mesh over the interval $0\le x\le L$

$$\phi_{\ell+1}=\phi_l+\Delta x\left.\frac{d\phi}{dx}\right|_l+\frac{\Delta x^2}{2}\left.\frac{d^2\phi}{dx^2}\right|_{\ell+\theta_1} \tag{3-5}$$

And therefore

$$\frac{d\phi}{dx}=\frac{\phi_{l+1}-\phi_l}{\Delta x}-\frac{\Delta x}{2}\frac{d^2\phi}{dx^2}\Big|_{l+\theta_1} \tag{3-6}$$

This leads to the so-called forward difference approximation of the first derivation of a function in which

$$\left.\frac{d\phi}{dx}\right|_l=\frac{\phi_{l+1}-\phi_l}{\Delta x^2} \tag{3-7}$$

The error E in this approximation can be seen to given by

$$E = -\frac{\Delta x}{2}\frac{d2\phi}{dx^2}\Big|_{l+\theta_l} \tag{3-8}$$

And as E is equal to a constant multiplied by Δx ,the error is $O(\Delta x)$, this is known as the order of the error.

The exact magnitude of the error cannot be obtained from this expression, as the actual value of ϕ_l is not given by Taylor's theorem, but it follows that

$$|E| \le \frac{\Delta x}{2}\max\left|\frac{d^2\phi}{dx^2}\right| \tag{3-9}$$

Figure (3-3) shows a graphical interpretation of the approximation that it was derived mathematically; the first derivative of $\phi(x)$ at $x = l$ is the slope of the tangent to the curve $y = \phi(x)$ at this point, that is the slope of this line approaches that of the line AB as the mesh spacing Δx gets smaller.

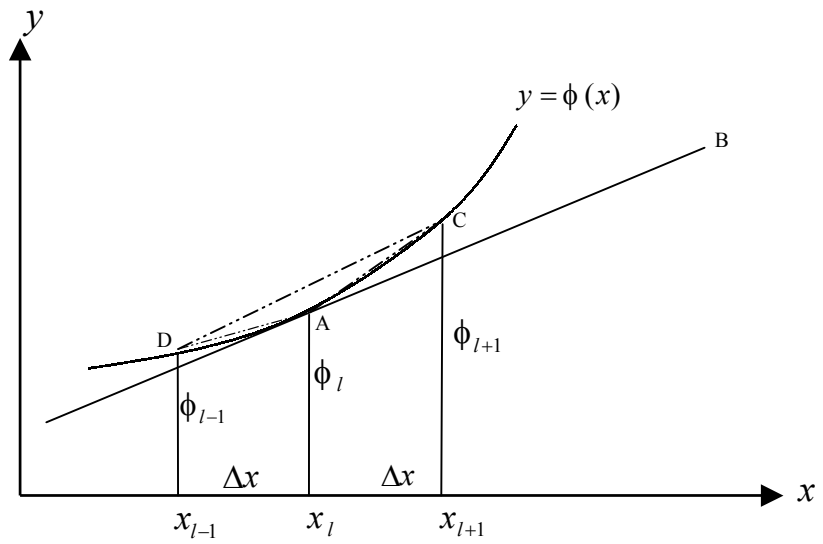

Figure 3-3: a graphical interpretation of some finite difference approximations to $\frac{d\phi}{dx}\Big|_l$. Forward difference-slope of AC; backward difference-slope of DA; central difference-slope of DC.

In a similar manner Taylor's series can be used to obtain

$$\phi_{l-1} = \phi_l - \Delta x \frac{d\phi}{dx}\bigg|_l + \frac{\Delta x^2}{2}\frac{d^2\phi}{dx^2}\bigg|_{l-\theta_2} \tag{3-10}$$

Where $0 \le \theta_2 \le l$ rewriting this expression in the form

$$\frac{d\phi}{dx} = \frac{\phi_l - \phi_{l-1`}}{\Delta x} + \frac{\Delta x}{2}\frac{d^2\phi}{dx^2}\Big|_{l-\theta_2} \tag{3-11}$$

It can produce the backward difference approximation

$$\frac{d\phi}{dx}\bigg|_l = \frac{\phi_\ell - \phi_{\ell-1}}{\Delta x} \tag{3-12}$$

The error E in this approximation is again $O(\Delta x)$ and now

$$E \le \frac{\Delta x}{2} \max \left| \frac{d^2\phi}{dx^2} \right| \tag{3-13}$$

The graphical representation of the backward difference approximation can be seen in Figure 3-3; the slope of the line AB is now approximated by the slope of the line AD.

In both the forward and the backward difference approximations the error is of the same order is, $O(\Delta x)$ however if we replace the expression of equation (3-5) and (3-10) by

$$\phi_{l+1} = \phi_l + \Delta x \frac{d\phi}{dx}\Big|_l + \frac{\Delta x^2}{2}\frac{d^2\phi}{dx^2}\Big|_l + \frac{\Delta x^3}{6}\frac{d^3\phi}{dx^3}\Big|_{l+\theta_3} \qquad 0 \le \theta_3 \le 1 \tag{3-14a}$$

$$\phi_{l-1} = \phi_l - \Delta x \frac{d\phi}{dx}\Big|_l + \frac{\Delta x^2}{2}\frac{d^2\phi}{dx^2}\Big|_l - \frac{\Delta x^3}{6}\frac{d^3\phi}{dx^3}\Big|_{l+\theta 4} \qquad 0 \le \theta_4 \le 1 \tag{3-14b}$$

Then a more accurate representation for the first derivative can be obtained by subtracting equation (3-14b) from equation (3-14a).

The resulting equation

$$\phi_{l+1} - \phi_{l-1} = 2\Delta x \frac{d\phi}{dx}\Big|_l + \frac{\Delta x^3}{6}\left(\frac{d^3\phi}{dx^3}\Big|_{l+\theta_3} + \frac{d^3\phi}{dx^3}\Big|_{l-\theta_4} \right) \tag{3-15}$$

Can be used to derive the (central difference approximation)

$$\frac{d\phi}{dx}\Big|_l = \frac{\phi_{l+1} - \phi_{l-1}}{2\Delta x^2} \tag{3-16}$$

And the error E in this approximation satisfies

$$E \le \frac{\Delta x^2}{6} \max \left| \frac{d^3\phi}{dx^3} \right| \tag{3-17}$$

As the error here is $O(\Delta x^2)$. This should now a better representation than either the forward or the backward difference approximation. This can again be see in the figure where the graphical interpretation is that were now approximating to the slope of the line AB by the slope of the line DC. Again adding the Taylor expansions.

$$\phi_{\ell+1} = \phi_l + \Delta x \frac{d\phi}{dx} + \left| {}_l \frac{\Delta x^2}{2} \frac{d^2\phi}{dx^2} \right|_l + \frac{\Delta x^3}{6} \frac{d^3\phi}{dx^3} \Big|_l + \cdots \quad \text{(3-18a)}$$

$$\phi_{l-1} = \phi_l - \Delta x \frac{d\phi}{dx} + \left| {}_l \frac{\Delta x^2}{2} \frac{d^2\phi}{dx^2} \right|_l - \frac{\Delta x^3}{6} \frac{d^3\phi}{dx^3} \Big|_l + \cdots \quad \text{(3-18b)}$$

We find that the terms involving the first and the third derivation disappear.

$$\frac{d^2\phi}{dx^2} = \frac{\phi_{l+1} - 2\phi_l + \phi_{l-1}}{\Delta x^2} - \frac{\Delta x^2}{24} \left(\frac{d^4\phi}{dx^4} \Big|_{l+\phi_5} + \frac{d^4\phi}{dx^4} \Big|_{l-\phi_6} \right) \quad \text{(3-19)}$$

And so we can approximate the second derivative by:

$$\frac{d^2\phi}{dx^2} = \frac{\phi_{l+1} - 2\phi_l + \phi_{l-1}}{\Delta x^2} \quad \text{(3-20)}$$

The error E in this approximation is $O(\Delta x^2)$ and satisfies [27]

$$E \le \frac{\Delta x^2}{12} \max \left(\frac{d^4\phi}{dx^4} \right) \quad \text{(3-21)}$$

3.6: Transformation Of Partial Differential Equation To Finite Difference Equation:

Since equation (3-3b) is:

$$\frac{\partial^2 T}{\partial x^2} + \frac{\partial^2 T}{\partial y^2} = \frac{1}{\alpha} \frac{\partial T}{\partial t}$$

This equation can be expressed in the finite difference form as:

$$\frac{T^{j}_{m+1,n} - 2T^{j}_{m,n} + T^{j}_{m-1,n}}{\Delta x^2} + \frac{T^{j}_{m,n+1} - 2T^{j}_{m,n} + T^{j}_{m,n-1}}{\Delta y^2} = \frac{1}{\alpha}\frac{T^{j+1}_{m,n} - T^{j}_{m,n}}{\Delta t} \qquad (3\text{-}23)$$

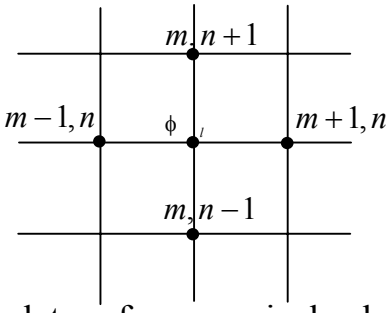

Figure 3-4: nomenclature for numerical solution of two-dimensional unsteady-state conduction

Thus if the temperature of the various nodes are known at any particular time the temperature after a time increment (Δt) may be calculated by writing an equation (22) for each node and obtaining the values of $\left(T^{j+1}_{m,n}\right)$. The procedure may be repeated to obtain the distribution after any desired number of time increment. If the increment of space coordinate are chosen such that $\Delta x = \Delta y$ and resulting equation for $\left(T^{j+1}_{m,n}\right)$becomes

$$T^{j+1}_{m,n} = \frac{\alpha \Delta t}{\Delta x^2}\left[T^{j}_{m+1,n} + T^{j}_{m-1,n} + T^{j}_{m,n+1} + T^{j}_{m,n-1}\right] + \left(1 - 4\frac{\alpha \Delta t}{\Delta x^2}\right)T^{j}_{m,n} \qquad (3\text{-}24)$$

$$T^{j+1}_{m,n} = Fo\left[T^{j}_{m+1,n} + T^{j}_{m-1,n} + T^{j}_{m,n+1} + T^{j}_{m,n-1}\right] + (1 - 4Fo)T^{j}_{m,n} \qquad (3\text{-}25)$$

Where fourier number may be defined as

$$Fo = \frac{\alpha \Delta t}{\Delta x^2} \qquad (3\text{-}26)$$

If the time increment are conveniently chosen so that

$$\frac{\alpha \Delta t}{\Delta x^2} = \frac{1}{4} \tag{3-27}$$

It is seen that the temperature of node Δx after a time increment is simply the arithmetic average of the four surrounding nodal temperature at the beginning of the time increment.

When a one-dimensional system involved the equation becomes

$$T_m^{j+1} = Fo\left(T_{m+1}^{j} + T_{m-1}^{j}\right) + \left[1 - 2Fo\right]T_m^{j} \tag{3-28}$$

and if the time and distance increments are chosen so that

$$\frac{\alpha \Delta t}{\Delta x^2} = \frac{1}{2} \tag{3-29}$$

The temperature of node (m) after the time increment is given as the arithmetic average of the two adjacent nodal temperatures
at the beginning of the time increment.

Note that if (Fo >½) in equation (3-28) the coefficient of $\left(T_m^{j}\right)$ becomes negative and a condition generated which will violate the second law of thermodynamics.

3.7: Stability Criteria Of The Finite Difference Equation

The restriction on the size of the fourier number is often referred to as (stability limit). This restriction automatically limits our choice of the Δt is established. If the fourier number exceeds $\left(\frac{1}{2}\right)$ for one-dimensional flow and exceeds $\left(\frac{1}{4}\right)$ for the two-dimensional flow .The solution for the temperature is said to be unstable.

$Fo \leq \frac{1}{2}$ For one-dimensional flow

$Fo \leq \frac{1}{4}$ For two-dimensional flow

3.8:Derivation of Temperature Distribution for Different Types Of Structure

Different types of structure such as (flat plate, T-element, stiffened structure plate) were taken to find the temperature distribution by using finite difference method. The assumptions were made to simplify the solution.

3.8.1:Derivation Of Temperature Distribution For Flat Plate

Consider the plate with relatively small thickness (d) as shown in the figure (3-5). The plate was subjected to convection from the upper and lower surface and to conduction from (x) and (y) directions.

After taking an elemental volume and make an energy balance the general partial differential equation was obtained. This equation was solved numerically by using Taylor Series therefore the temperature distribution over the whole plate is calculated.

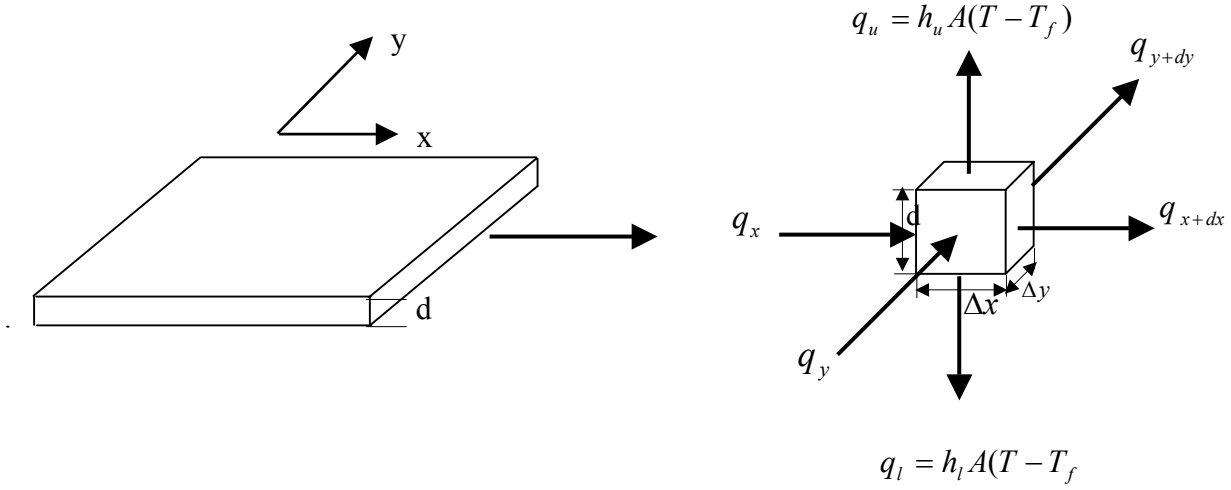

Figure 3-5: Energy balance on flat

Making the following assumptions to simplify the solution.

1. The plate will assumed to have relatively small thickness (d) Therefore conduction through the thickness is zero.
2. There is no heat generation.

3. Constant thermal conductivity.
4. Radiation effect will be neglected
5. Grid spaces are equal.

Make an energy balance on the elemental volume

Energy Balance: Energy in = Energy out + internal energy

Energy Balance: Energy in = Energy out + internal energy

$$q_x + q_y = q_{x+dx} + q_{y+dy} + hA\left(T - T_f\right) + h_l A\left(T - T_f\right) + \frac{\partial E}{\partial t} \qquad (3\text{-}30)$$

Where:

h_u = Convection heat transfer coefficient for upper surface

h_l = Convection heat transfer coefficient for lower surface

Since

$$q_x = -KA\frac{dT}{dx}$$

$$q_{x+dx} = q_x + \frac{\partial}{\partial x}q_x dx$$

$$q_y = -KA\frac{dT}{dy}$$

$$q_{y+dy} = q_y + \frac{\partial}{\partial y}q_y dy$$

$$\frac{\partial E}{\partial t} = \rho c d(\Delta x \Delta y)\frac{\partial T}{\partial t}$$

Substitute these quantities into equation (3-30)

$$q_x + q_y = q_x + \frac{\partial q_x}{\partial x}dx + q_y + \frac{\partial q_y}{\partial y}dy + h_u A\left(T - T_f\right) + h_l A\left(T - T_f\right) + \frac{\partial E}{\partial t} \qquad (3\text{-}31)$$

$$K(d\Delta y)\frac{\partial^2 T}{\partial x^2}dx + K(d\Delta x)\frac{\partial^2 T}{\partial y^2}dy - h_u(\Delta x\Delta y)\left(T - T_f\right) - h_l(\Delta x\Delta y)\left(T - T_f\right) = \frac{\partial E}{\partial t} \qquad (3\text{-}32)$$

$$K(d\Delta y)\frac{\partial^2 T}{\partial x^2}dx + K(d\Delta x)\frac{\partial^2 T}{\partial y^2}dy - h_u(\Delta x\Delta y)\left(T - T_f\right) - h_l(\Delta x\Delta y)\left(T - T_f\right) = \rho\, c\, d\,(\Delta x\Delta y)\frac{\partial T}{\partial t} \qquad (3\text{-}33)$$

Divide equation (3-33) by $\Delta x\, \Delta y$

$$Kd\left[\frac{\partial^2 T}{\partial x^2}+\frac{\partial^2 T}{\partial y^2}\right]-\left(h_u+h_l\right)\left(T-T_f\right)=\rho\, c\frac{\partial T}{\partial t}d \tag{3-34}$$

Divide equation (3-34) by Kd will obtain

$$\frac{\partial^2 T}{\partial x^2}+\frac{\partial^2 T}{\partial y^2}-\frac{h}{Kd}\left(T-T_f\right)=\frac{1}{\alpha}\frac{\partial T}{\partial t} \tag{3-35}$$

Where:

$$\alpha = \frac{K}{\rho\, c}$$

$$h = h_u + h_L$$

When transform this partial differential equation to finite difference equation obtain

$$\frac{T^j_{m+1,n}-2T^j_{m,n}+T_{m-1,n}}{\Delta x^2}+\frac{T^j_{m,n+1}-2T^j_{m,n}+T^j_{m,n-1}}{\Delta y^2}-\frac{h}{Kd}(T^j_{m,n}-T_f)=\frac{1}{\alpha}\frac{T^{j+1}_{m,n}-T^j_{m,n}}{\Delta t} \tag{3-36}$$

Put $\Delta x=\Delta y$

$$\frac{\alpha\,\Delta t}{\Delta x^2}\left[T^j_{m+1,n}-4T^j_{m,n}+T^j_{m-1,n}+T^j_{m,n+1}+T^j_{m,n-1}\right]-\alpha\,\Delta t\frac{h}{Kd}(T^j_{m,n}-T_f)=T^{j+1}_{m,n}-T^j_{m,n} \tag{3-37}$$

Multiply the second term by $\frac{\Delta x^2}{\Delta x^2}$

$$Fo\left[T^j_{m+1,n}-4T^j_{m,n}+T^j_{m-1,n}+T^j_{m,n+1}+T^j_{m,n-1}\right]-R\,Fo\,Bi\,(T^j_{m,n}-T_f)=T^{j+1}_{m,n}-T^j_{m,n} \tag{3-38}$$

Where:

$$Fo=\frac{\alpha\,\Delta t}{\Delta x^2}$$

$$Bi=\frac{h\Delta x}{K}$$

$$R=\frac{\Delta x}{d}$$

Then the general finite difference equation will be

$$T_{m,n}^{j+1} = (1 - 4Fo - RFoBi)T_{m,n}^{j} + Fo(T_{m+1,n}^{j} + T_{m-1,n}^{j} + T_{m,n+1}^{j} + T_{m,n-1}^{j}) + RFoBiT_f \quad (3\text{-}39)$$

And the stability limit will be:

$$1 - 4\,Fo - RFo\,Bi \geq 0$$

Or multiply by (-1)

$$-1 + 4\,Fo + RFo\,Bi \leq 0$$

Then by add (1) to both sides results

$$4\,Fo + RFo\,Bi \leq 1$$

$$\therefore\ Fo\,(4 + R\,Bi) \leq 1 \qquad \text{(Stability limit for flat plate)} \qquad (3\text{-}40)$$

3.8.2:Derivation Of Temperature Distribution For T-element Structure

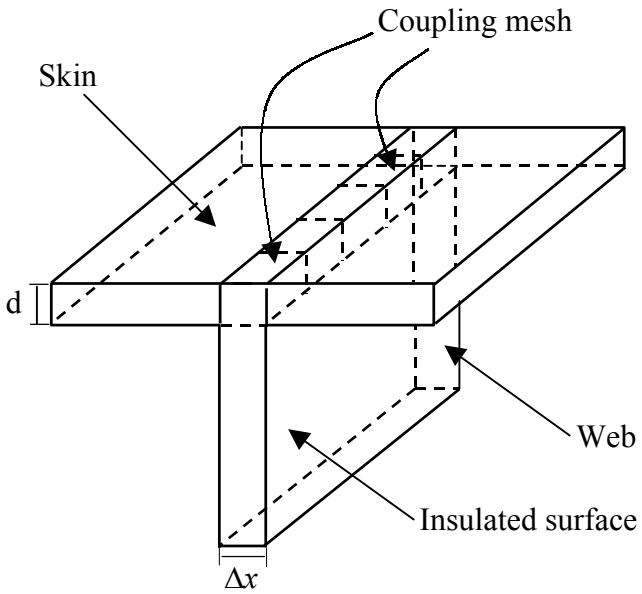

Figure 3-6: T-element structure

In order to find the temperature distribution of the T-element (skin –web) structures placed in three dimensions as shown in the figure. Energy balance on the elemental volume was made in three regions skin, web and the coupling mesh (which is the region of contact between the two plates) then applying finite difference method therefore three cases will be made to find the temperature distribution on the skin of (T-element).

The same assumptions for flat plate are used also. The surface of the web will be insulated therefore there is no convection on the web.

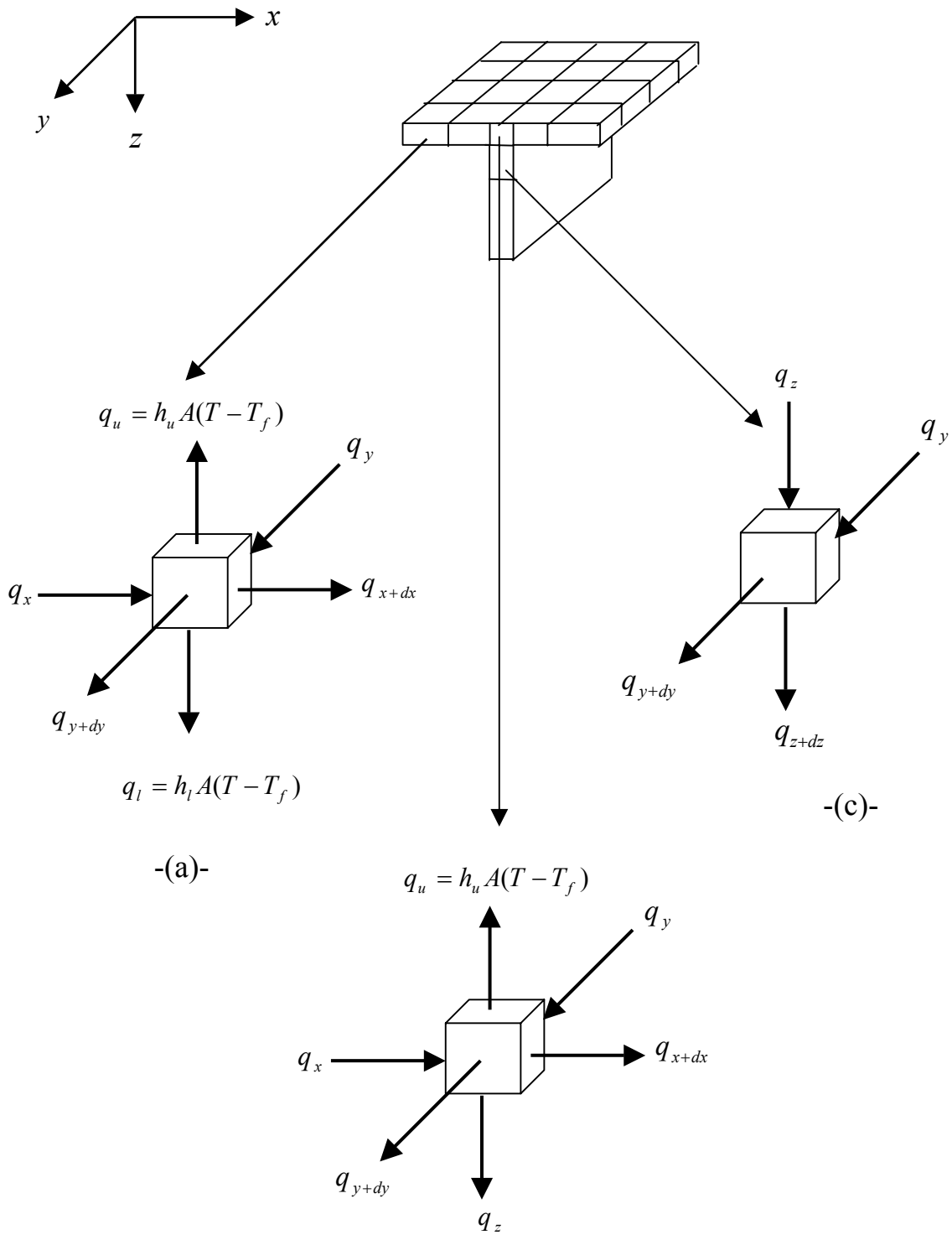

Figure 3-7: Energy balance for (T-element) structure

Figure 3-7 shows the energy balance on the elemental volume for (T-element) in three regions therefore three equations were derived to find the temperature distribution in the skin of (T-element).

a-Derivation Of Temperature Distribution For The Skin of T-element

The same equations in (3.9.1) for flat plate were used to find the temperature distribution for the skin of T-element.

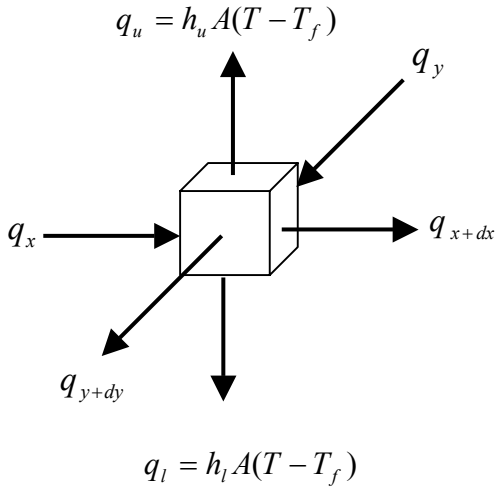

-a-

b-Derivation of Temperature Distribution For The coupling Mesh

Making an energy balance on the elemental volume of the coupling mesh to obtain the partial differential equation and this will be solved by using finite difference method.

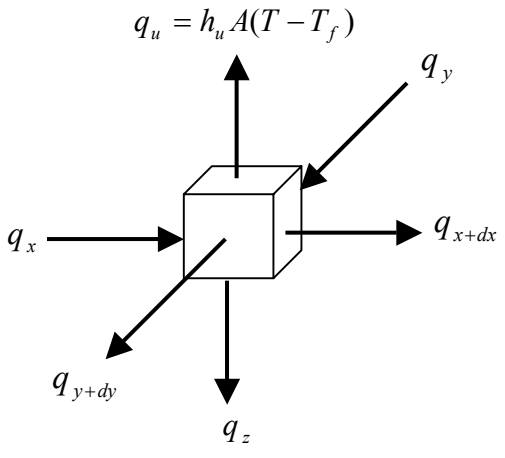

-b-

Applying energy balance:

Energy in = Energy out + internal energy

$$q_x + q_y = q_{x+dx} + q_{y+dy} + q_z + q_u + \frac{\partial E}{\partial t} \tag{3-41}$$

$$q_x + q_y = q_x + \frac{\partial}{\partial x} q_x dx + q_y + \frac{\partial}{\partial y} q_y dy + q_z + q_u + \frac{\partial E}{\partial t} \tag{3-42}$$

$$K(d\Delta y)\frac{\partial^2 T}{\partial x^2}\Delta x + K(d\Delta x)\frac{\partial^2 T}{\partial y^2}\Delta y - q_z - q_u = \frac{\partial E}{\partial t} \tag{3-43}$$

$$K(d\Delta y)\frac{\partial^2 T}{\partial x^2}\Delta x + K(d\Delta x)\frac{\partial^2 T}{\partial y^2}\Delta y + K(\Delta x\Delta y)\frac{\partial T}{\partial z} - h(\Delta x\Delta y)(T - T_f) = \rho\, c(\Delta x\Delta y d)\frac{\partial T}{\partial t} \tag{3-44}$$

Divide equation (3-44) by $(\Delta x \Delta y)$

$$Kd\,\frac{\partial^2 T}{\partial x^2} + Kd\,\frac{\partial^2 T}{\partial y^2} + K\,\frac{\partial T}{\partial z} - h_u(T - T_f) = \rho\, c(d)\frac{\partial T}{\partial t} \tag{3-45}$$

And the partial differential equation will be

$$\frac{\partial^2 T}{\partial x^2} + \frac{\partial^2 T}{\partial y^2} + \frac{1}{d}\frac{\partial T}{\partial z} - \frac{h_u}{dK}(T - T_f) = \frac{1}{\alpha}\frac{\partial T}{\partial t} \tag{3-46}$$

Transform this differential equation to finite difference equation obtain:

$$\frac{T^j_{m+1,n} - 2T^j_{m,n} + T_{m-1,n}}{\Delta x^2} + \frac{T^j_{m,n+1} - 2T^j_{m,n} + T^j_{m,n-1}}{\Delta y^2} + \frac{1}{d}\frac{T^j_{l+1} - T_l{}^j}{\Delta z} - \frac{h_u}{kd}(T^j_{m,n} - T_f) = \frac{1}{\alpha}\frac{T^{j+1}_{m,n} - T^j_{m,n}}{\Delta t} \tag{3-47}$$

Since $\Delta x = \Delta y$

$$\frac{\alpha\,\Delta t}{\Delta x^2}\left[T^j_{m+1,n} - 4T^j_{m,n} + T^j_{m-1,n} + T^j_{m,n+1} + T^j_{m,n-1}\right] + \frac{\alpha\,\Delta t}{\Delta z}\frac{1}{d}(T^j_{l+1} - T_l{}^j) - \alpha\,\Delta t\frac{h}{Kd}(T^j_{m,n} - T_f) = T^{j+1}_{m,n} - T^j_{m,n} \tag{3-48}$$

Multiply the second term by $\frac{\Delta z}{\Delta z}$ and the third term by $\frac{\Delta x^2}{\Delta x^2}$

$$Fo\left[T^j_{m+1,n} - 4T^j_{m,n} + T^j_{m-1,n} + T^j_{m,n+1} + T^j_{m,n-1}\right] + R_z\, Fo_z(T^j_{l+1} - T^j_{m,n}) - R\, Fo\, Bi_u(T^j_{m,n} - T_f) = T^{j+1}_{m,n} - T^j_{m,n} \tag{3-49}$$

$$T_{m,n}^{j+1} = (1-4Fo-RFo-RFoBi_u)T_{m,n}^{j} + Fo(T_{m+1,n}^{j} + T_{m-1,n}^{j} + T_{m,n+1}^{j} + T_{m,n-1}^{j}) + R_z Fo_z T_{l+1}^{j} + RFoBi_u T_f \quad (3\text{-}50)$$

And the stability limit is

$$\therefore Fo(4+R+RBi_u) \le 1 \quad \text{Stability limit of equation (b)} \quad (3\text{-}51)$$

c-Derivation Of Temperature Distribution For The Web of T-element

Making an energy balance on the elemental volume of the web

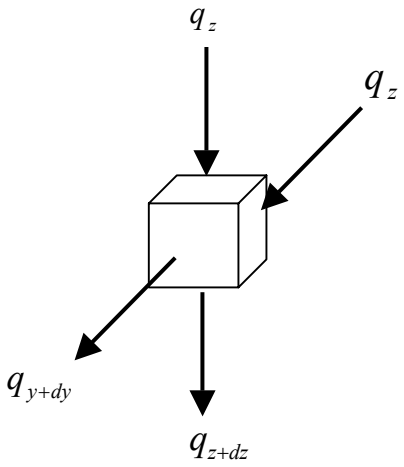

-c-

Energy Balance: Energy in = Energy out + internal energy

$$q_y + q_z = q_{y+dy} + q_{z+dz} + \frac{\partial E}{\partial t} \quad (3\text{-}52)$$

$$q_y + q_z = q_y + \frac{\partial}{\partial y} q_y dy + q_z + \frac{\partial}{\partial z} q_z dz + \frac{\partial E}{\partial t} \quad (3\text{-}53)$$

$$k(\Delta z \Delta x)\frac{\partial^2 T}{\partial y^2}\Delta y + k(\Delta x \Delta y)\frac{\partial^2 T}{\partial z^2}\Delta z = \rho\, c(\Delta x \Delta y \Delta z)\frac{\partial T}{\partial t} \quad (3\text{-}54)$$

Divide equation (3-54) by $k(\Delta x \Delta y \Delta z)$ will get the partial differential equation.

$$\frac{\partial^2 T}{\partial y^2} + \frac{\partial^2 T}{\partial z^2} = \frac{1}{\alpha}\frac{\partial T}{\partial t} \quad (3\text{-}55)$$

Transforming it to finite difference equation:

$$\frac{T_{n+1,l}^{j}-2T_{n,l}^{j}+T_{n-1,l}^{j}}{\Delta y^{2}}+\frac{T_{n,l+1}^{j}-2T_{n,l}^{j}+T_{n,l-1}^{j}}{\Delta z^{2}}=\frac{1}{\alpha}\frac{T_{n,l}^{j+1}-T_{n,l}^{j}}{\Delta t} \tag{3-56}$$

$$T_{n,l}^{j+1}=\frac{\alpha\,\Delta t}{\Delta z^{2}}\left[T_{n+1,l}^{j}+T_{n-1,l}^{j}+T_{n,l+1}^{j}+T_{n,l-1}^{j}\right]+\left(1-4\frac{\alpha\,\Delta t}{\Delta z^{2}}\right)T_{n,l}^{j} \tag{3-57}$$

$$T_{n,l}^{j+1}=Fo_{z}\left[T_{n+1,l}^{j}+T_{n-1,l}^{j}+T_{n,l+1}^{j}+T_{n,l-1}^{j}\right]+\left(1-4Fo_{z}\right)T_{n,l}^{j} \tag{3-58}$$

And the stability limit is:

$Fo\le\frac{1}{4}$ (Stability limit of equation (c))

3.8.3:Derivation Of Temperature Distribution For Stiffened Structure Plate.

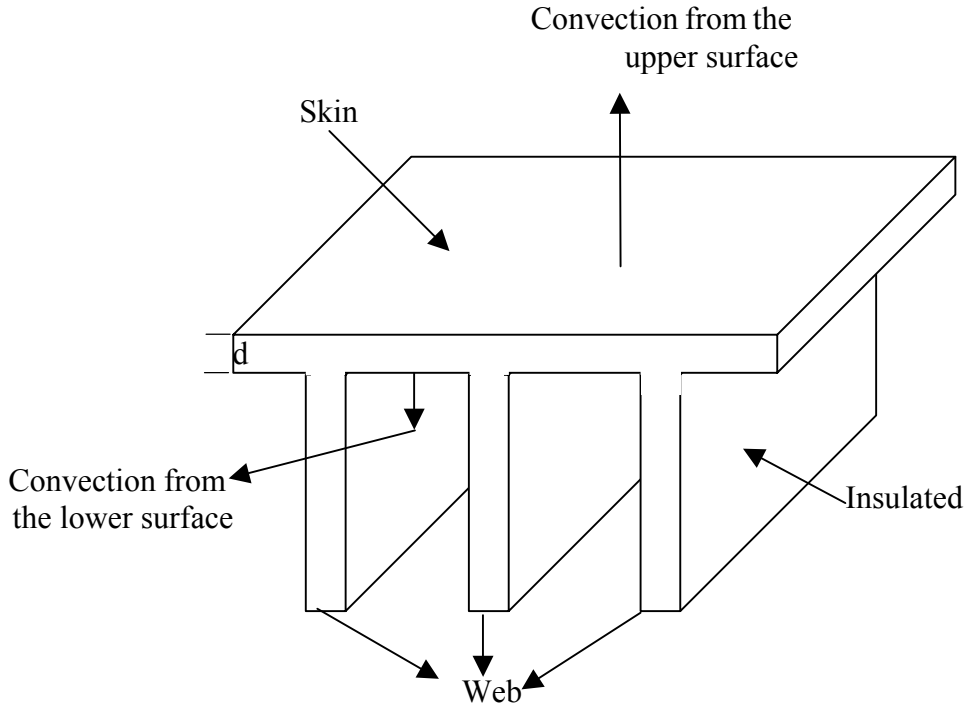

Figure 3-8: stiffened structure plate

Stiffened structure plate consists of skin with multi branches (web) as shown in fig 3-8. The same approach of (T-element) will be used to find the temperature distribution but here there are three web therefore equation (3-50) applied at the three coupling mesh. Also all the surfaces of the web are insulated and the same boundary conditions of (T-element) are applied.

3.9: Radiation Heat Transfer

In contrast to the mechanisms of conduction, where energy transfer through a material medium is involved. Heat may also be transferred through regions where a perfect vacuum exists. The mechanism in this case is electromagnetic radiation. Which is propagated as a result of temperature difference: this is called thermal radiation.

Thermodynamic considerations show that an ideal thermal radiator or black-body will emit energy at a rate proportional to the fourth power of the absolute temperature of the body and directly proportional to its surface area. Thus

$$q_{emitted} = \sigma A T^4 \qquad (3\text{-}59)$$

Where σ is the proportionality constant and is called Stefan–Boltzman constant with the value of 5.669×10^{-8} W/m².k^4 .

Equation (3-59) is called the Stefan – Boltzman law of thermal radiation and it applies only to black bodies.0.

Equation (3-59) governs only radiation emitted by a black body. The net radiant exchange between two surfaces will be proportional to the difference in absolute temperatures to the fourth power

$$\frac{q_{net\,exchange}}{A} \propto \sigma (T_1^4 - T_2^4) \qquad (3\text{-}60)$$

3.10:Radiation In an Enclosure

A simple radiation problem is encountered we have a heat – transfer surface at temperature T_1 completely enclosed by a much larger surface maintained at T_2

The net exchange can be calculated with

$$q = \varepsilon_1 \sigma A_1 (T_1^4 - T_2^4) \qquad (3\text{-}61)$$

Values of ε are given in Ref. [26]

3.11:Computer Programs

Matlab is a powerful computing system for handling the calculation involved in scientific and engineering problems [28]. The constants will be entered at the beginning of the program that includes the thickness of the plate; initial temperature, boundary temperatures, and convection heat transfer coefficient. When running the program the number of nodes and material properties will be entered as an input to the program to get the temperature distribution as an output. The flow chart of the program is shown below. The computer program shown in appendix A

Flow Chart Of The Program

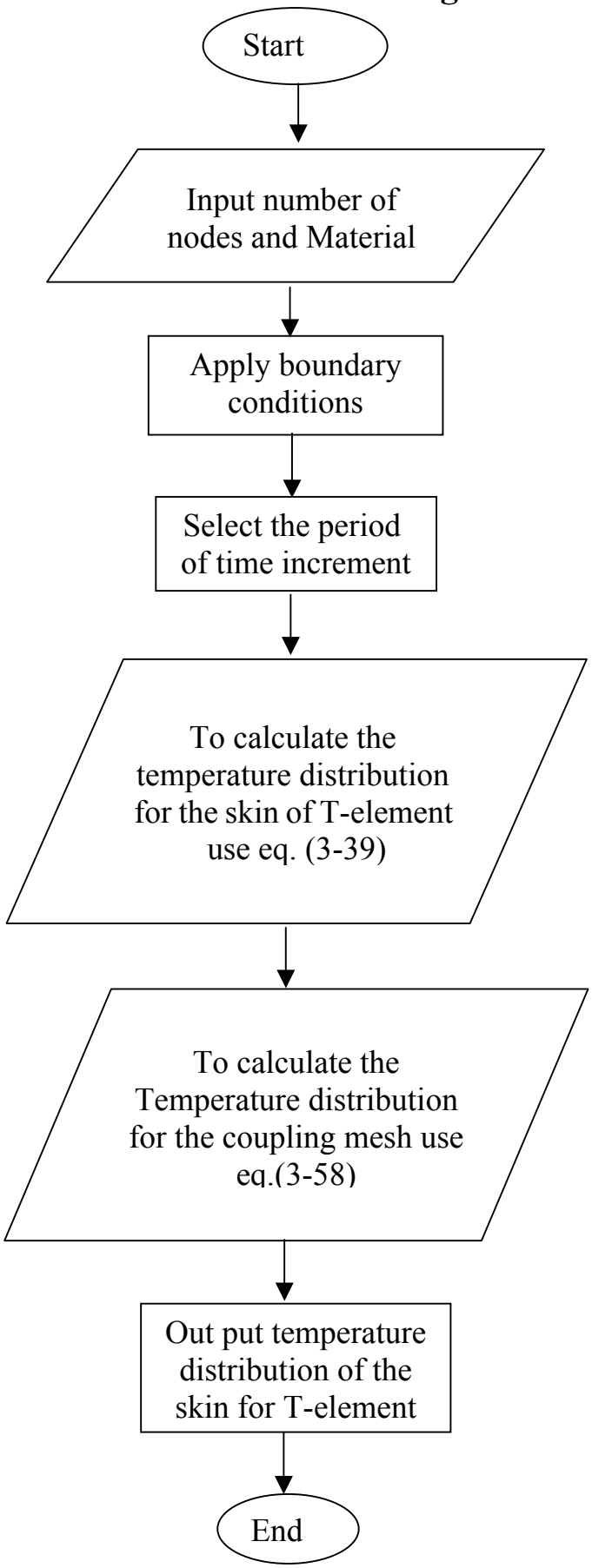

Chapter Two

Literature Survey

The development of numerical techniques such as finite difference and finite element method has enabled engineers to solve extremely complex physical phenomena for a variety of boundary conditions and material properties. In the following paragraph some of the works are reviewed.

Casagrande[6] presented a complete discussion on the use of the flownet technique for predicting seepage through earth structures, originally developed by Forchheimer.

Cassagrande divided the soil into two parts, the soil below the water table and the soil above the water. The assumption was made that water only flowed below the water table. The flownet method was used extensively in geotechnical practice.

A large amount of research was conducted in the 1970's for development of numerical models for predicting heat flow in soils. This occurred in response to several proposals for construction of oil and gas pipelines in Northern Canada and Alaska. The models needed to account for the latent heat effects as the pore water changes phases.

Bhattacharya [7] and **Lick [8]** applied the improved finite-difference method (FDM) to time-dependent heat conduction problems with step-by step computation in the time domain. The finite-element method (FEM) based on variation principle, was used by

Gurtin [9] to analyze the unsteady problem of heat transfer**. Emery** and **Carson [10]** as well as **Visser [11]** applied variational formulations in their finite-element solutions of non stationary temperature distribution problems.

Bruch and **Zyvoloski [12]** solved the transient linear and non-linear two-dimensional heat conduction problems using the finite-element weighted residual process.

Chen et al [13] successfully applied a hybrid method based on the Laplace transform and the FDM to transient heat conduction problems

The disadvantages of these methods are the complicated procedure, need for large storage and long computation time.

Wang et al [14] used the implicit spline method of splitting to solve the two and three-dimensional transient heat conduction problems. The method is applied to homogeneous and isotropic solid. A cubic spline method has been developed in the numerical integration of partial differential equations since the pioneering work of **Rubin and Graves [15]**, and **Rubin and Khosla [16]**. This method provides a simple procedure, small storage, short computation time, and a high order of accuracy. Furthermore, the spline method has a direct representation of gradient boundary condition.

Zbynek Svoboda [17] studied the numerical model for the analysis of the combined Convective-conductive heat transfer in the building components has been developed. Presented model is based on the partial differential equation for the two dimensional steady-state heat transport caused by conduction and convection. The finite element method was used to obtain the numerical solution of the governing equation. The general finite element formulation was derived by means of the Petrov-Galerkin approach. The developed computer program was used to study one typical lightweight building wall construction. The results of simulation demonstrate that the lightweight constructions insulated with permeable mineral wool are very sensitive to the convective heat transfer.

William R. Hamburgen [18] studied optimal finned heat sinks. In a multi-board computer system, the volume allocated for heat removal is often a significant fraction of the total system volume. Cooling requirements can thus impact performance, reliability, cost, acoustic noise, and floor space. This work addresses the volume costs or space requirements for removing heat with optimally designed finned heat sinks. Simple formulas applicable to both gas and liquid cooling problems provide upper bounds on the thermal resistance of an optimal heat sink, without explicitly designing the part. Conservative junction temperature estimates can thus be made without detailed design.

S.Oktay[19] Also, on- off cycle of an electronic product creates high temperature variations. Heat generated inside the Electronic Package can be harmful to the components and to the Printing Wring Board itself. Generated heat must be removed. Heat removal from the electronic system becomes more important as chip power increases. One of the most common methods for heat removal is forced convection of air through heat generators.

Andrej V. Cherkaev and Thomas C. Robbins [20] studied optimization of heat conducting structures they considered various structures designed to shield temperature sensitive devices from the heat generated by a given distributed source. These structures should redistribute the heat and control the total heat dissipation, in order to maintain a prescribed temperature profile in a certain region of the domain. They assume there are several materials available, each with different constants of heat conductivity, and that they are allowed to mix them arbitrarily. It is known that optimal structures consist of laminate composites that are allowed to vary within the design domain. The paper discusses optimal distributions of these composites for different settings of the problem that

include: prescribed volume fractions and various types of boundary conditions. They solve the problem numerically using the method of finite elements.

Manfred Gilli and Evis.Këllezi [21] they investigate computational and implementation issues for the valuation of options on three underlying assets, focusing on the use of the Finite difference methods. They demonstrate that implicit methods, which have good convergence and stability properties, can now be implemented efficiently due to the recent development of techniques that allow the efficient solution of large and sparse linear systems. In the trivariate option valuation problem, they use nonstationary iterative methods (also called Krylov methods) for the solution of the large and sparse linear systems arising while using implicit methods. Krylov methods are investigated both in serial and in parallel implementations. Computational results show that the parallel implementation is particularly efficient if a fine spatial grid is needed.

It is generally accepted that the dimensionality of the problem is a nontrivial issue. Up to a dimension of three, methods like the finite differences or the finite elements can still be used. With a greater number of state variables, Monte Carlo (one of the optimization method) is thought to be the only way out. For bivariate problems finite difference methods, both explicit and implicit have been successfully implemented.

A.N. Pavlov and S.S. Sazhin [22] They carried out a conservative finite difference method and its application for the analysis of a transient flow around a square prism

Detailed results of numerical calculations of transient, 2D incompressible flow around and in the wake of a square prism at Re = 100, 200 and 500 are presented. An implicit finite difference Operator -splitting method, a version of the known simplec-like method on a staggered grid, is

described. Appropriate theoretical results are presented. The method has second-order accuracy in space, conserving mass, momentum and kinetic energy. A new modification of the multi grid method is employed to solve the elliptic pressure problem. Calculations are performed on a sequence of spatial grids with up to 401* 321 grid points, at sequentially halved time steps to ensure grid-independent results. Three types of flow are shown to exist at Re = 500: a steady-state unstable flow and two which are transient, fully periodic and asymmetric about the center line but mirror symmetric to each other. Discrete frequency spectra of drag and lift coefficients are presented.

Dr. Jalal M. Jaleel [23] studied body – fitted coordinate system in solving temperature distribution problem in cooling turbine blade. In finite difference formulation, introduction of the body – fitted coordinate system has made it possible by using finite difference method in many situations with complicated geometry. The method of body fitted coordinate system was used in predicting the temperature distribution in complicated shapes such as a turbine blade. The method shows excellent agreement compared with finite elements results. It seems an efficient, flexible tool for solving partial differential equation in complicated geometry in fluid and solid mediums.

David R Buttsworth [24] studied a Finite Difference Routine for the Solution of Transient One Dimensional Heat Conduction Problems with Curvature and Varying Thermal Properties.

The implicit finite difference routine was developed for the solution of transient heat flux problems that are encountered using thin film heat transfer gauges in aerodynamic testing. The routine allows for curvature and varying thermal properties within the substrate material. The routine was written using MATLAB script. It has been found that errors, which

arise due to the finite difference approximations, are likely to represent less than 1% of the inferred heat flux for typical transient test conditions.

He was concluding the finite difference routine provides a convenient way of accounting for influence of curvature and temperature-dependent thermal properties within the substrate used for transient heat flux experiments.

Heat flux errors, which arise due to the finite difference approximations, are likely to represent less than 1% of the inferred heat flux for typical transient test conditions. This is an acceptable level of accuracy since uncertainties in the temperature measurements and the actual thermal properties of the substrate are likely to represent a far greater contribution to the overall accuracy of the heat flux measurements.

From the previous researchers it was seen that Battacharya, Lick and Dr.Jalal used finite difference method for solving their heat conduction problems at different boundary conditions while Carson and Visser, Zbynek Svoboda used finite element method also there is other researchers used another numerical technique mentioned above.

In this thesis it is used transient finite difference method for solving the temperature distribution on different type of finned plate structure.

Reference

1- James Suces " Heat Transfer " Wm.c Brown Publishers USA, 1985

2- Nogotov E.F, "Application of Numerical Heat transfer" Hemisphere, McGraw- Hill, New York 1978

3- Craig S. Collier " stiffness, thermal expansion, and thermal Bending Formulation of stiffened, fiber- Reinforced composite panels " AIAA / ASME/AHS / ACS 34th structures, Dynamic & Material conference 1993

4-Lewis R, W, and Morgan, K. "Numerical Methods In heat Transfer" John Wiley New York 1985 Volume 3

5- William S. Janna "Engineering Heat Transfer" Six Edition

6-Jason S. Pentland " Use of a General Partial Differential Equation Solver for Solution of Mass and Heat Transfer Problems in Geotechnical Engineering" University of Saskatchewan, Canada 1999

7-Bhattacharya, M.C**.**, 1985, an explicit Conditionally Stable Finite Difference Equation for Heat Conduction Problems. Int. J. Numer. Methods Eng., vol. 21, pp. 239-265

8-Lick, W., 1985, Improved Difference Approximation to the Heat Equation, Int. J. Numer. Methods Eng., vol. 21, pp. 1957-1969,

9-Gurtin, M. E., 1964, Variational Principles for linear Initial-Value Problems, Q. Appl. Math., vol. 22, pp. 252-256,

10- Emery, A. F. and Carson, W.W., 1971, An Evaluation of the Use of the Finite Element Method in the Computation of Temperature, ASME J. Heat Transfer, vol. 39, pp. 136-145

11-Visser, W., 1965, A finite Element Method for the Determination of Non-Stationary Temperature Distribution and Thermal Deformations, Proc. Conference on Matrix Methods in Structural Mechanics, pp. 925-943, Air Force Institute of Technology,

Wright Patterson Air Force Base, Dayton, Ohio
12-Bruch, J.C. and Zyvolovski, G., 1974, Transient two-dimensional Heat Conduction Problems Solved by the Finite Element Method, Int. J. Numer. Methods Eng., vol. 8, pp. 481-494
13- Chen H-K and Chen C-K, 1988, Application of Hybrid Laplace Transform/Finite Difference Method to Transient Heat Conduction Problems, Numerical Heat Transfer, vol. 14, pp. 343-356
14- Wang, S.P., Miao, Y. and Miao, Y.M., 1990, An Implicit Spline Method of Splitting for the Solution of Multi-Dimensional Transient Heat Conduction Problems, Proc., Advanced Computational Methods in Heat Transfer, vol. 1, pp. 127-137
15. Rubin, S.G. And Graves, R.A., 1975, Cubic Spline Approximation for Problems in Fluid Mechanics, NASA TR R-436 18.
16-Rubin, S.G. and Khosla, P.K., 1976, Higher Order Numerical Solutions Using Cubic Splines, AIAA J., vol. 14, pp. 851-858.
17-Zbynek Svoboda ”the analysis of the convective-conductive heat transfer in the building constructions” **166** 29 Prague 6 1991

18-William R. Hamburgen” Optimal Finned Heat Sinks” Digital Equipment Corporation Western Research Laboratory 100 Hamilton Avenue Palo Alto, CA 94301 28 October 1986
19-Oktay, R.J.Hanneman, and A. Bar-Cohen, 1986”High Heat From A Small Package”, Mech. Eng., vol 108, no. 3, pp.36-42
20-Cherkaev, Andrej **V.,** 1999, Variational Approach to Structural Optimization. Structural Dynamic Systems, Computational Techniques and Optimization, 9, 199--236.
21- Manfred Gilli and Evis.Këllezi “solving finite difference schemes arising in trivariate option pricing” university of Geneva, 1221 Geneva, Switzerland

22-A.N. Pavlov and S.S. Sazhin "A conservative finite difference method and its application for the analysis of a transient flow around a square prism" International Journal of Numerical Methods for Heat & Fluid Flow, Vol. 10 No. 1, 2000, pp. 6-46MCB University Press, 0961-5539

23-Dr. Jalal M. Jaleel "body – fitted coordinate system in solving temperature distribution problem in cooling turbine blade" engineering and technology vol.17 no.9, 1998

24-David R Buttsworth "A Finite Difference routine for the solution of Transient One dimensional heat conduction Problems with Curvature and Varying Thermal Properties" Faculty of Engineering & Surveying University of Southern Queensland November 2001

25- Saeed Moarani "Finite Element Analysis", Hall, Inc, 1999

26- Holman, J.P "Heat Transfer", McGraw - Hill Book Company, New York, 8th edition 1989

27- Morgan" Finite elements and approximation" a Wiley-Interscience publication John Wiley and sons 1983

28-Brian D.Hahn "Essential matlab for scientists and Engineers" John Wiley and sons Inc. New York 1997

بسم الله الرحمن الرحيم

"سبحانك لا علم لنا الا ما علمتنا انك انت العزيز الحكيم"

اتقدم بعظيم شكري وفـائـق امتنـ ـاني لاستـ ـاذي الفـاضـ ـل **(أ. د. خالد عبد الحميد)** المشرف على اعداد هذا البحث لما ابداه من مساعدة كبيرة وجهود مخلصة من اجل انجاز هذا البحث بصورته الحالية هذه الحصيلة وهذا الجهد، ارجو من الله عز وجل ان يمن عليه بدوام الصحة كما اوجه شكري وعرفاني الى رئيـ ـس قسم الهندسـ ـة الميكـانيكيـة **(أ. د. هشام محمد توفيق)** وجميع الاساتذة والمدرسين في القسم.

الى من دلّني على طريق المعرفة واناره لي ... أبي.

الى من عبّد لي درب الحياة فسهلها لي ... أمي.

الى من شجعاني للأستمرار في درب العلم الشائك ... أخواتي.

فائق شكري وتقديري الى طالب الدكتوراه (علي حسين) للمساعدة الكبيرة التي قدمها لي .

وختاماً اقدم شكري الجزيل الى كل اصدقائي وزملائي في مرحلة البحث.

NUMERICAL STUDY OF TEMPERATURE PROFILE FOR FINNED PLATE WITH DIFFERENT BOUNDARY CONDITIONS

A Thesis

Submitted to the College of Engineering of

Al-Nahrain University in Partial Fulfillment of the

Requirements for the Degree of Master of Science

in Mechanical Engineering

By

MUSTAFA FIKRAT ASKER

(B.Sc.2001)

Rabia-Althani **1425**

May **2004**

Abstract

The present study has been carried out to investigate numerical study of temperature profile for finned plate with different boundary conditions.

For many practical heat transfer problems it is not possible to obtain a solution by means of analytical techniques. Instead, Solving them requires the use of numerical methods, which in many cases allow such problems to be solved quickly. Often an engineer can easily see the effect of changes in parameter when modeling a problem numerically.

The numerical techniques used in the present study are based on transient finite difference. An advantage of this method is that it provides a good physical understanding and allows for simple incorporation of modification such as heat source. Explicit method of finite difference is simple and straightforward approach and resulting system of algebraic equations is very easy to solve.

The transient surface temperature distribution is determined for different types of structures subjected to convection and conduction.

The radiation effect is neglected. Taylor series was used to solve the partial differential equation obtained from energy balance.

Different types of structures (flat plate, T-element, stiffened structure plate) were taken to find the temperature distribution.

The coupling mesh developed in this thesis in T-element and stiffened structure plate to know the effect of temperature distribution on these structures that may cause a thermal stress and may lead to a failure of the structure.

Computer program (Matlab6.1) was used to calculate the temperature distribution on these structures.

It is found that the variation of thermal conductivity has an effect on the shape of the concaveness of the temperature profile and the global minimum of the curve varied with the increasing of the time increment.

Contents

Abstract **I**

Contents III

Nomenclature **V**

Chapter One: Introduction 1

Chapter Two: Literature Survey 6

Chapter Three: Numerical Analysis

3.1:Numerical Method 12

3.2:Finite Difference Method in Steady-State Heat Transfer by Conduction 13

3.3: Finite Difference Method in Unsteady-State Heat Transfer by Conduction 14

3.4: Derivation Of The General Heat-Conduction Equation 15

3.5: The Finite Difference Approximation Of Derivative 17

3.6: Transformation Of Partial Differential Equation To Finite Difference Equation 21

3.7:Stability Criteria Of the Finite Difference Equation 23

3.8:Derivation of Temperature Distribution for Different Types Of Structure 24

3.8.1:Derivation Of Temperature Distribution For Flat Plate 24

3.8.2:Derivation Of Temperature Distribution For T-element Structure 28

3.8.3:Derivation Of Temperature Distribution For Stiffened Structure Plate 34
3.9:Radiation Heat Transfer 35
3.10:Radiation In an Enclosure 35
3.11:Computer Programs 36
Chapter Four: Calculation, Results And Discussion
4.1:Calculations 38
4.1.1:For Flat Plate 38
4.1.2:For T-element 40
4.2:Results and Discussion 45
4.2.1:Flat Plate 45
4.2.2:T-element 46
4.2.3:Stiffened Structure Plate 47
4.3:Contour Plots 47
4.4:Radiation Effects 50
Chapter Five: Conclusions And Recommendations For Future Work
5.1: Conclusions 73
5.2: Future Work 74
References 75
Appendix
Appendix A

Nomenclature

Symbol	Definition	Units
A	Cross section Area	m^2
Bi	Biot number	___
c	Specific heat	kJ / kg. C°
d	Thickness of the plate	m
E	Energy	W
Fo	Fourier number	___
h	Convection heat transfer coefficient	W/m^2. C°
h_u	Convection heat transfer coefficient for the upper surfaces of the plate	W/m^2. C°
h_l	Convection heat transfer coefficient for the lower surfaces of the plate	W/m^2. C°
L	Length of the plate	m
q	Heat transfer rate	W
m,n	Denotes nodal position in numerical solution	___
R	Ratio	___
T	Temperature	C°
T_f	Fluid temperature	C°
t	Time	S
α	Thermal diffusivity	m^2/s
σ	Stefan- Boltzman constant	$W/m^2.k^4$
ρ	Density	kg/m^3
ε	Emissivity	___
Δ	Small increment	___

الخلاصة

انجز البحث الحالي في الدراسة العددية لتوزيع درجات الحرارة على السطوح المزعنفة وبظروف حدودية مختلفة. انه من غير الممكن الحصول على حل لعدد من المسائل التطبيقية لانتقال الحرارة باستخدام الطريقة التحليلية. فبدلاً من ذلك يتطلب حلها استخدام التحليل العددي الذي قد يؤدي الى سرعة ايجاد الحلول لبعض الحالات وقد يرى المهندس احياناً تأثير التغير في العوامل حين صياغة المسألة عددياً.

ان الظروف العددية المستخدمة في هذه الدراسة مبنية على الفروقات العددية المحددة، ان فائدة هذه الطريقة تكمن في اعطاء الفهم الفيزيائي الجيد وتسمح ببساطة الارتباط للتحويرات مثل المصدر الحراري. ان طريقة الفروقات المحددة بسيطة ومباشرة وتكون المعادلات الجبرية الناتجة منها سهلة الحل. تم احتساب التوزيع السطحي اللحظي لدرجات الحرارة لانواع مختلفة في الهياكل التي تعرضت الى الحمل والتوصيل مع اهمال التأثير الاشعاعي واستخدمت متسلسلة تايلور لحل المعادلات الثنائية الجزئية التي تم الحصول عليها من توازن الطاقة الحرارية.

استخدمت انواع مختلفة من الهياكل (صفيحة مستوية، صفيحة ذات شكل حرف T ، وصفيحة مقوى) لايجاد التوزيع الحراري .

ان الوصلة الرابطة المستخدمة في هذا البحث للصفيحة ذي الشكل T والصفيحة المقوى هو لمعرفة تأثير توزيع درجات الحرارة في هذين الهيكلين الذي قد يسبب اجهادات حرارية قد تؤدي الى اخفاق الهيكل.

تم استخدام البرنامج الحاسوبي (MATLAB 6.1) لحساب توزيع درجات الحرارة في هذه الهياكل. لقد وجد ان التغير في مقدار التوصيلية الحرارية له تأثير على التقعر لمظهر توزيع درجة الحرارة وان النقطة الصغرى للمنحني تتغير مع زيادة الفترة الزمنية .

دراسة عددية لتوزيع درجات الحرارة في الصفيحة المزعنفة بظروف حدودية مختلفة

رسالة

مقدمة الى كلية الهندسة في جامعة النهرين وهي جزء من متطلبات نيل درجة ماجستيرعلوم في الهندسة الميكانيكية

من قبل المهندس

مصطفى فكرت عسكر

(بكالوريوس 2001)

ربيع الثاني 1425 هـ

مايس 2004 م